FINAL PROJECT REPORT

U.S. Department of Transportation
Federal Aviation Administration

Form Approved:
O.M.B. No. 2120-0559
9/30/2013

PART I - PROJECT IDENTIFICATION INFORMATION

1. Institution and Address	2. FAA Program	3. FAA Award Number
	4. Award Period From To	5. Cumulative Award Amount

6. Project Title

PART II - SUMMARY OF COMPLETED PROJECT (For Public Use)

PART III - TECHNICAL INFORMATION (For Program Management Uses)

1. ITEM (Check appropriate blocks)	NONE	ATTACHED	PREVIOUSLY FURNISHED	TO BE FURNISHED SEPARATELY TO PROGRAM	
				Check (X)	Approx. Date
a. Abstracts of Theses					
b. Publication Citations					
c. Data on Scientific Collaborators					
d. Information on Inventions					
e. Technical Description of Project and Results	■				
f. Other (specify)					

2. Principal Investigator/Project Director Name (Typed)	3. Principal Investigator / Project Director Signature	4. Date

FAA Form 9550-5 (03-03) Supersedes Previous Edition

Part III – Technical Information

Thesis Abstracts

Drew Weibel (S.M., 2018)
Naphthalenes have been identified as a precursor to aviation-attributable black carbon (BC) emissions. Given its 1-2 vol% concentration in jet fuel, there are several refining processes that may be used to remove naphthalene without impacting its ability to meet specification. This study evaluates the economic feasibility of jet fuel naphthalene removal (via hydro-treatment or extractive distillation). We develop a stochastic discounted cash flow model based on the retrofit of existing US refineries with naphthalene removal systems, and compute costs from both societal and market perspectives. We find that the US-average cost premium over the market price of jet fuel is 4.7 cents/liter for hydro-treatment and 3.1 cents/liter for extractive distillation. Considered from a societal perspective, costs are 1.7 cents/liter and 2.4 cents/liter, respectively. The costs incurred by small refineries can be up to 270% higher than the national average. Hydro-treatment costs are found to be more sensitive to upfront capital investment, while extractive distillation costs are more sensitive to crude price volatility. Additional jet fuel life cycle greenhouse gas emissions from naphthalene removal are $3.35 gCO_2e/MJ$ and $3.12 gCO_2e/MJ$ for hydro-treatment and extractive distillation, respectively. Coupled with analysis of the impacts of reduced aviation-attributable BC emissions, this work can provide a comprehensive comparison to alternative emission reduction pathways.

Lukas Brink (S.M., 2020)
Aircraft NO_x, CO and soot emissions contribute to climate change and lead to negative air quality impacts. With the aim of quantifying the effects of fuel composition on NO_x, CO and soot emissions, a combustor model named Pycaso is developed. The combustor model consists of a 0D/1D reactor network, coupled with a soot model. The model predicts NO_x, CO and soot emissions at sea level conditions for a CFM56-7B engine using conventional jet fuel. The model matches existing methods to predict cruise NO_x emissions within 5% and cruise CO emissions within 30%. It is shown that the volume – and thus time – over which secondary air is mixed with the fuel-air mixture in the combustor is the most important factor in determining the magnitudes of the modeled emissions. The sensitivity of modeled NO_x and CO emissions to thrust at thrust settings below 15% is shown to be the consequence of "cold" unburned fuel entering the secondary zone of the combustor. The model is used to assess two possible emission mitigation solutions: removing naphthalene from jet fuel and replacing conventional jet fuel with 50:50 biofuel blends. The removal of naphthalene through hydrotreating is found to lead to mean reductions in soot emissions of 15% [12%-20%] for mass and 9% [5%-19%] for number. The range captures variations in engine operating conditions, soot model configurations and compositions of the baseline jet fuel. Similarly, the removal of naphthalene through extractive distillation reduces soot mass emissions by 32% [29%-48%] and number emissions by 23% [14%-45%]. The mean reductions associated with using 50:50 biofuel blends are 43% [34%-59%] for soot mass and 35% [14%-45%] for soot number. Using biofuel blends is also predicted to result in a reduction in NO_x emissions of 5% [4%-7%] and a 3% [2%-4%] decrease in CO emissions.

Mengjie Liu (Ph.D., 2020)
Polycyclic aromatic hydrocarbons (PAHs), large molecules comprised of multiple aromatic rings like anthracene or pyrene, are a notable intermediate and byproduct in combustion or pyrolysis of hydrocarbon fuels. On their own, they have been shown to pose a significant health risk, with certain PAHs being linked to increased cancer risk in humans. In addition, PAHs are known to play an important role as building blocks towards larger particles, known as soot or black carbon, which contribute a significant fraction of atmospheric $PM_{2.5}$ pollution (particulate matter with diameters under 2.5 μm). These particulates pose additional health risks and can also contribute to global climate change via radiative forcing. This motivates interest in understanding the chemical pathways leading to the formation of these PAHs, which could inform better models to predict PAH emissions and optimize methods to reduce their formation.

This thesis presents methods to improve the capabilities of automatic mechanism generation software in modeling the complex chemistry involved in PAH formation. In particular, it focuses on the Reaction Mechanism Generator (RMG) software, an open-source package developed primarily in Python. RMG automatically identifies species and reactions which are relevant at conditions of interest to aid construction of detailed mechanisms, but it has not been previously applied for PAH chemistry. To do so, new algorithms were developed to improve treatment of aromaticity and chemical resonance to better reflect the true behavior of molecules within the limitations of programmatic representations. The effect of polycyclic ring strain on parameter estimation was also investigated, highlighting challenges in capturing 3D conformational effects using the existing estimation frameworks and methods to address them.

These improvements to fundamental algorithms play an important role in how thermochemical and kinetic parameters are estimated. The combined utility of these developments is demonstrated by the generation of a detailed mechanism for modeling PAH formation up to pyrene in acetylene pyrolysis, which represents an important milestone in RMG capabilities. Analysis of the model provides insight into the relative contributions of various PAH formation pathways, revealing that hydrogen abstraction, acetylene addition pathways are the key contributors to PAH formation in this system.

Publication Citations

Papers

Liu, Mengjie & Green, William H. (2019). Capturing aromaticity in automatic mechanism generation software. Proceedings of the Combustion Institute 37(1), 575–581. *https://doi.org/10.1016/j.proci.2018.06.006*

Theses

Weibel, Drew (2018). Techno-economic assessment of jet fuel naphthalene removal to reduce non-volatile particulate matter emissions. S.M. Thesis, Massachusetts Institute of Technology. *https://hdl.handle.net/1721.1/124174*

Brink, Lukas (2020). Modeling the impact of fuel composition on aircraft engine NO_x, CO and soot emissions. S.M. Thesis, Massachusetts Institute of Technology. *https://hdl.handle.net/1721.1/129181*

Liu, Mengjie (2020). Predictive modeling of polycyclic aromatic hydrocarbon formation during pyrolysis. Ph.D. Thesis, Massachusetts Institute of Technology. *https://hdl.handle.net/1721.1/129925*

Data on Scientific Collaborators

Principal Investigator:	Prof. Steven Barrett
Co-Principal Investigator:	Dr. Raymond L. Speth
Co-Investigators:	Prof. William Green Dr. Sebastian Eastham Dr. Jayant Sabnis Randall Field
Postdoctoral Associates:	Dr. Agnes Jocher Dr. Mica Smith
Graduate Students:	Drew Weibel Lukas Brink Mengjie Liu

Project 039 Naphthalene Removal Assessment

Massachusetts Institute of Technology

Project Lead Investigator

Prof. Steven R. H. Barrett
Professor of Aeronautics and Astronautics
Department of Aeronautics and Astronautics
Massachusetts Institute of Technology
77 Massachusetts Avenue – Bldg. 33-316
Cambridge, MA 02139
(617)-452-2550
sbarrett@mit.edu

University Participants

Massachusetts Institute of Technology
- PI(s): Prof. Steven R. H. Barrett and Dr. Raymond Speth (Co-PI)
- FAA Award Number: 13-C-AJFE-MIT
- Period of Performance: July 8, 2016 to February 28, 2021
- Task(s):
    1. Preliminary screening of naphthalene removal refining processes
    2. Calculation of process requirements and fuel composition effects for selected refining processes
    3. Estimate capital and operating costs of naphthalene removal
    4. Develop kinetic model of polycyclic aromatic hydrocarbon (PAH) formation with fuel-composition effects
    5. Compare kinetic model results to LFP/PIMS experimental data
    6. Evaluate relationship between PAH formation and aircraft particulate matter (PM) emissions
    7. Calculate air quality and climate impacts of naphthalene removal
    8. Conduct integrated cost-benefit analysis of impacts of naphthalene removal in the United States

Investigation Team

- Prof. Steven Barrett (MIT) served as PI for the A39 project as head of the Laboratory for Aviation and the Environment. Prof. Barrett both coordinates internal research efforts and maintains communication among investigators in the various MIT research teams mentioned below.
- Dr. Raymond Speth (MIT) served as co-PI for the A39 project. Dr. Speth directly advised students performing research in the Laboratory for Aviation and the Environment, with a focus on assessment of naphthalene removal refinery options; climate and air quality modeling; and fuel alteration life-cycle analysis. Dr. Speth also coordinated communication with FAA counterparts.
- Prof. William Green (MIT) served as a co-investigator for the A39 project, as head of the Green Research Group. Prof. Green advised students on work in the Green Research Group focused on computer-aided chemical kinetic modeling of PAH formation.
- Mr. Randall Field (MIT) is the Executive Director of the MIT Energy Initiative and was a co-investigator of the A39 project. Drawing upon his experiences as a business consulting director at Aspen Technology Inc., Mr. Field provided mentorship to student researchers in the selection and assessment of naphthalene removal refining options and process engineering at large.
- Mr. Drew Weibel (MIT) was a graduate student researcher in the Laboratory for Aviation and the Environment. Mr. Weibel was responsible for conducting selection and assessment of naphthalene removal refining options; calculation of refinery process requirements and fuel composition effects from selected processes; estimation of capital and operating costs of naphthalene removal processes; air quality and climate modeling; and integrated cost-benefit analysis.
- Mr. Lukas Brink (MIT) was a graduate student researcher in the Laboratory for Aviation and the Environment. Mr. Brink was responsible for the development of a combustor model quantifying the effect of naphthalene removal on soot emissions, and the use of this model to assess air quality and climate impacts of naphthalene removal.

- Dr. Mica Smith (MIT) was a postdoctoral associate in the Green Research Group. Ms. Smith was responsible for the experimental measurements being used for the validation of the chemical kinetic mechanisms.
- Dr. Agnes Jocher (MIT) was a postdoctoral associate in the Green Research Group. Ms. Jocher was responsible for evaluating microphysical models that link the presence of PAH molecules to the formation of soot particles and for providing modeling expertise in combining these models with the kinetic models being developed.

Project Overview

The composition of aviation fuels affects the formation of pollutants that contribute to climate change and reduced air quality that leads to adverse health impacts including increased risk of premature mortality. The objective of this project was to assess the societal costs and benefits of removing naphthalenes from jet fuel produced in the United States. Removal of naphthalene by extractive distillation is found to be less expensive than the use of hydrotreatment. Hydrotreatment has the additional effect of removing sulfur from the fuel, while fuel processed by extractive distillation has larger reductions in nvPM emissions. The largest environmental benefits come from reductions in air quality damages due to sulfur emissions, although the removal of sulfur also results in a net warming effect on the climate. Climate benefits due to reductions in nvPM emissions are mainly associated with reductions in contrail radiative forcing. However, this benefit is more than offset by the increased CO_2 emissions required for the naphthalene removal processes. These results suggest that naphthalene removal on a nationwide basis is unlikely to be cost beneficial using either extractive distillation or hydrotreatment. However, naphthalene removal could be beneficial under certain circumstances, for example, if applied to fuels used at individual airports with particular air quality concerns, or if used at times and locations where the formation of warming contrails is most likely.

References

Brem, B.T., Durdina, L., Siegerist, F., Beyerle, P., Bruderer, K., Rindlisbacher, T., Rocci-Denis, S., Andac, M.G., Zelina, J., Penanhoat, O., & Wang, J. (2015). Effects of fuel aromatic content on nonvolatile particulate emissions of an in-production aircraft gas turbine. Environmental Science and Technology 49 13149–57

Moore, R.H., Shook, M., Beyersdorf, A., Corr, C., Herndon, S., Knighton, W.B., Miake-Lye, R., Thornhill, K.L., Winstead, E.L., Yu, Z., Ziemba, L.D. & Anderson, B.E. (2015). Influence of jet fuel composition on aircraft engine emissions: A synthesis of aerosol emissions data from the NASA APEX, AAFEX, and ACCESS missions. Energy Fuels 29 2591–600

Task 1 - Preliminary Screening of Naphthalene Removal Refining Processes

Massachusetts Institute of Technology

Objective

Naphthalene is present in varying levels in straight-run crude oil distillation cuts used to produce jet fuel and is currently not targeted for removal in treatments used to meet industry standard fuel specifications. As a result, reducing the naphthalenic content in jet fuel entails the introduction of an additional refinery treatment process. The objective of this task is to identify suitable refinery processes that can be used to remove or convert naphthalenes. Once identified, data for key refining process parameters will be collected to inform future cost estimation of applying the selected processes for jet fuel naphthalene removal.

Research Approach

Introduction

Refining processes, and chemical processes at large, are focused on subjecting chemical species to various environments to allow for conversion, combination, separation, etc. in order to produce useful, increased value products. When considering removal of a chemical component from a mixture, say naphthalenic species from a kerosene feed, a process designer must consider unique properties shared by the chemical component that allow for its conversion, combination, separation, etc. without affecting the underlying mixture.

While naphthalenes are not currently targeted for removal to meet industry standards, there are several mature refining technologies that, once tuned, can complete this reduction/removal with high efficiency. We select suitable, readily accessible refining technologies for the removal of naphthalenes from the U.S. jet pool. Our focus is on technologies currently used in industry, in order to provide possible policies that could be implemented in the near term.

Methods

To select a number of refining processes for the large-scale removal of naphthalenes from the U.S jet fuel pool, we complete a literature review of current technologies, qualitative evaluation of those technologies in terms of their applicability of naphthalene removal, the scope of economic and process data available, and the level of naphthalene removal achievable. Particular attention will be given to preserving non-naphthalenic aromatics, since reducing the amount of these components would limit the capacity to blend paraffinic alternative jet fuels while still meeting minimum requirements for aromatics.

In order to evaluate each candidate process, we will leverage existing literature to estimate the utility (process fuel, electricity, hydrogen, etc.) requirements for each process the effect on the composition of the resulting jet fuel, and the capital costs of new refinery equipment required. We will include the effects of any pre-processing that may be required. We will then compare processes side by side in order to demonstrate the trade-offs associated with naphthalene removal at the refinery.

As a by-product of analyzing a range of different refining pathways, we will be able to assess the tradeoffs associated with different levels of naphthalene removal. Combined with later work in development of a relationship between jet fuel composition and PAH formation, we will be able to assess the level of severity in which naphthalene's should be removed, in order to optimize costs and benefits.

Results

This task was concluded with the selection of extractive distillation and selective hydro-treating as candidate refinery processes for the large-scale removal of naphthalenes from the U.S. jet fuel pool.

Naphthalenes are unsaturated, double ring aromatic species which may contain alkylated or impurity groups. They are most readily removed via conversion to mono-aromatic or saturated species – via hydrogen addition or carbon removal – or separated based on polarity. A desired refinery process would remove naphthalenic species with high efficiency, not affect the remaining aromatic content, produce minimal changes to other fuel properties, and produce limited emissions and economic impact; removal of other impurities (sulfur, nitrogen, etc.) is a bonus. A list of potential refining processes is shown in Figure 1 (Gary et al., 2007).
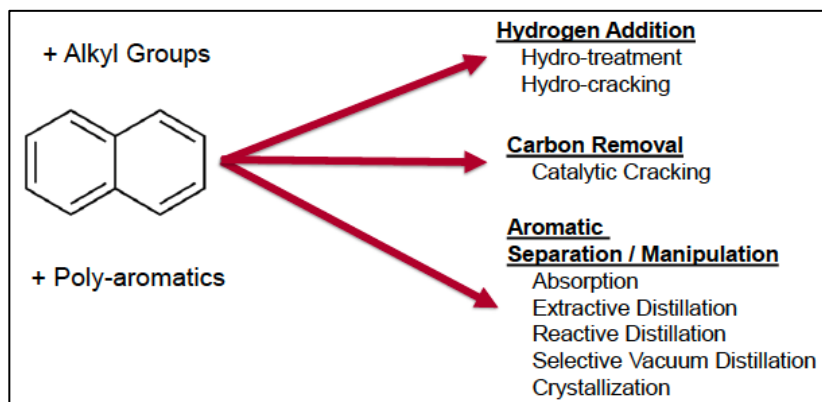

Figure 1: Categories of potential processes for naphthalene removal

As noted, there are three families of processes pertinent to the removal of naphthalenes; conversion by hydrogen addition (saturation), conversion by carbon removal (cracking), or aromatic separation. Hydrogen addition and aromatic separation are often used as finishing processes and can operate under mild conditions. Carbon removal, on the other hand, is often associated with molecular cracking, has the potential to radically convert the feed, is associated with the production of olefins, and often cannot break apart stable aromatic rings. As a result, only hydro-conversion and aromatic separation processes were considered.

Hydro-conversion processes are a family of refining units that react a petroleum feed with gaseous hydrogen at elevated temperatures and pressures to saturate – and in severe processes, crack – hydrocarbon molecules. Hydro-treating is a mild hydro-conversion finishing process used to remove impurities and saturate olefin and aromatic species. Selective hydro-treating for the conversion of naphthalenes is a viable process candidate because the second ring of naphthalenic species will tend to be fully saturated prior to the saturation of mono-aromatic species. Due to the relative selectivity of fuel

components, we also expect desulfurization and di-nitrogenation to occur. As a result, with a robust catalyst selection and finely tuned process parameters, we expect a selective hydro-treating process could reduce/remove naphthalenes by converting them to mono-aromatics with little change to the overall aromatic content and other fuel characteristics, and with reasonable hydrogen requirements (Fahim et al., 2009).

Separation processes provided a separation of mixture components about some defining species characteristic such as weight, size, polarity, etc. Extractive distillation provides a separation of petroleum components based on polarity, by introducing a heavy, high-boiling point polar solvent to the feed. Highly polar component (including all aromatic and impurity containing species), will bind to the solvent and be separated from other species based on weight. The solvent is then separated using by simple distillation. Finally, mono-aromatic and naphthalene species can be roughly separated in a second distillation step, the prior cut being returned to the feed. Extractive distillation, while less common for feed mixture separations, was identified as a second candidate for naphthalene removal from the U.S. jet fuel pool (Meyers, 2004).

After selection of extractive distillation and selective hydro-treating as candidate refining processes for the removal/reduction of naphthalene from the U.S. jet fuel pool, further details were collected on each process to define their offsite needs and fuel composition impacts. Table 1 shows relevant process requirements and fuel effects.

Table 1: Process requirements and fuel impacts for hydro-treatment and extractive distillation

Process Name	Hydro-Treatment	Extractive Distillation
Description	Naphthalenes are hydrogenated to mono-aromatic and cyclo-paraffinic components.	All aromatics are separated via a polar solvent. Mono-aromatics are separated from naphthalenes via distillation and blended back into the jet fuel product
Process Type	Conversion (H_2 addition)	Aromatic Separation
Existing Uses	Desulfurization, impurity removal, aromatic hydrogenation	Separation of polar feed components, BTX separation
Removal of Naphthalenes	Assumed 95% efficient	Assumed 95% efficient
Effect on Mono-Aromatics	Limited (<10%) hydrogenation	Fully separated; fraction returned to product can be controlled
Impurity Removal	S, N removal to <50 ppm	Small removal of S, N impurities
Supporting Processes Req'd	Hydrogen production, Sulfur gas removal, sulfur post-treatment, steam generation and cooling facilities	Naphthalene / mono-aromatic post distillation, steam generation and cooling facilities
Process Innovation Req'd	Minimal required. Very similar to existing units	Efficient solvent with impurity (S,N) resiliency

Milestone
This task was concluded with the selection of extractive distillation and selective hydro-treating as candidate refinery processes for the large-scale removal of naphthalenes from the U.S. jet fuel pool. The results were described in a presentation provided to the FAA on February 28th, 2017.

Major Accomplishments
During this period, two refining processes – selective hydro-treating and extractive distillation – were chosen as suitable candidates for large-scale naphthalene removal from the U.S. jet fuel pool. A summary of this work is contained in the deliverable 1 presentation provided to the FAA on February 28th, 2017.

Publications

- Weibel, Drew (2018). Techno-economic assessment of jet fuel naphthalene removal to reduce non-volatile particulate matter emissions. S.M. Thesis, Massachusetts Institute of Technology. *https://hdl.handle.net/1721.1/124174*

Outreach Efforts
- ASCENT advisory board presentations/posters (April 2017, September 2017, April 2018)

Student Involvement
Drew Weibel, Master's student in the Laboratory for Aviation and the Environment worked directly with Prof. Steven Barrett and Dr. Raymond Speth to conduct the research objectives of Task 1.

References
Gary, J. H., Handwerk, G. E., & Kaiser, M. J. (2007). *Petroleum Refining: Technology and Economics* (Fifth Edition). CRC Press.
Fahim, M. A., Al-Sahhaf, T., & Elkilani, A. (2009). *Fundamentals of Petroleum Refining*. Elsevier Science.
Meyers, R. (2004). *Handbook of Petroleum Refining Processes* (Third Edition). McGraw-Hill.

Task 2 - Calculation of Process Requirements and Fuel Composition Effects for Selected Refining Processes
Massachusetts Institute of Technology

Objective
In Task 1, selective hydro-treating and extractive distillation were selected as candidate refinery process for large-scale reduction or removal of naphthalene from the U.S. jet fuel pool. In addition, data was collected regarding the offsite (or the supporting process) requirements and fuel composition effects of each process.

The objective of this task is to continue quantitative analysis of both processes in order to develop simplified estimation models of process requirements and fuel composition effects. The result of this task will be the cost estimation for individual selective hydro-treating and extractive distillation refinery units, modelled as brown-field additions to existing refinery operations.

Research Approach
Methods
Based on the collection of process parameters as part of Task 1, utility requirements and capital cost data were collected for distillate hydro treating, extractive distillation, and their supporting processes. The supporting processes of selective hydro-treating are steam methane reforming for hydrogen production, amine separation for hydrogen sulfide separation from off-gasses, and the Claus process for sulfur recovery. Because these supporting processes are often connected to several units at a refinery, they are costed based on both the size of the modelled refinery and the capacity of the modelled hydro-treatment unit. The sole supporting process for extractive distillation is post-distillation.

In order to calculate the net present value of an added refinery finishing process for the reduction/removal of naphthalene from jet fuel, the methods described by Gary et al. (2007) are adopted. Fixed capital investment was estimated from the desired process capacities and the collected cost data. Operating cost was calculated as a function of the fixed costs, and as a function of the utility requirements and estimated utility costs (depicted in Figure 2). Catalyst/Solvent and process water utility costs are assumed constant (Gary et al. 2007, Peters et al., 2003). Historical and predicted natural gas and electricity prices, by U.S. census region, are taken from the U.S. Energy Information Administration. Using an auto-regressive – moving average (ARMA) model, calibrated to the predicted trend and historical price variations, natural gas and electricity prices are estimated stochastically. The net present value is then calculated using a Discounted Cash Flow Rate of Return (DCFRoR) model over the lifetime of the process unit. A discount factor of 2.74%, based on the 20-year constant maturity rate, is used for the estimated cost to society.
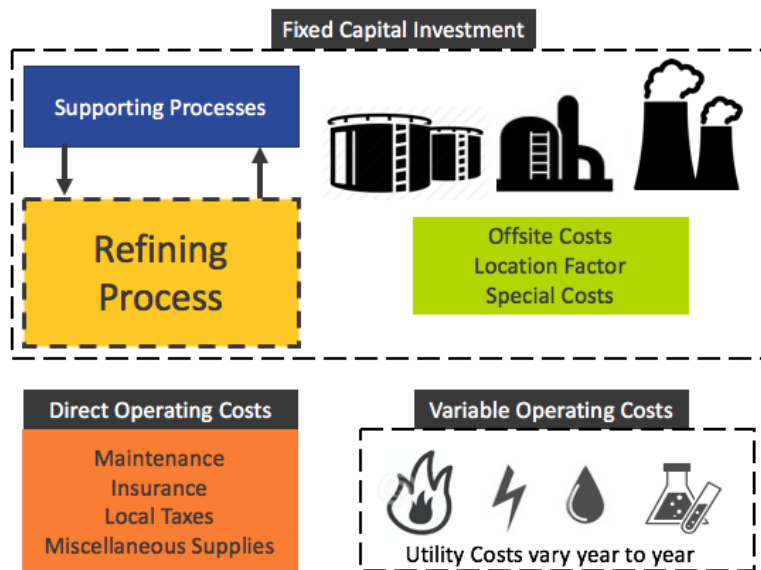
Figure 2: Schematic of factors affecting costs of refinery processes

Results
The model successfully estimates the cost of the reduction or removal of naphthalene from U.S. jet fuel via operation of an additional finishing process (either selective hydro-treating or extractive distillation) at U.S. refineries. Preliminary cost data is presented in the deliverable 3 presentation provided to the FAA on August 31st, 2017.

Milestone
This work was completed in August 2017 and summarized in the Deliverable 1-3 presentation provided to FAA on August 31st, 2017.

Major Accomplishments
During this period, a simplified model was created for the purpose of cost estimation of individual selective hydro-treating and extractive distillation process units. This included effects on fuel composition, utility requirements, and estimated costs over the lifetime of the unit. Results collected from the discounted cash flow model are presented as the net present value of the unit over its lifetime. A summary of this work is contained in Deliverable 1-3, provided to the FAA on August 31st, 2017.

Publications
Theses
- Weibel, Drew (2018). Techno-economic assessment of jet fuel naphthalene removal to reduce non-volatile particulate matter emissions. S.M. Thesis, Massachusetts Institute of Technology. *https://hdl.handle.net/1721.1/124174*

Outreach Efforts
- ASCENT advisory board presentations/posters (September 2017, April 2018, October 2018)
- Presentation at CRC Aviation Meeting (May 2018) titled "Naphthalene Removal Assessment: Cleaning up Jet Fuel for Reduced Environmental Impacts"
- Presentations at Aviation Emissions Characterization (AEC) Roadmap Annual Meeting (May 2018, May 2020)

Student Involvement
Drew Weibel, Master's student in the Laboratory for Aviation and the Environment, worked directly with Prof. Steven Barrett and Dr. Ray Speth to conduct the research objectives of this task.

References
Gary, J. H., Handwerk, G. E., & Kaiser, M. J. (2007). *Petroleum Refining: Technology and Economics* (Fifth Edition). CRC Press.

Peters, M. S., Timmerhaus, K. D., West, R. E. (2003). *Plant Design and Economics for Chemical Engineers*. (Fifth Edition). McGraw-Hill.

Task 3 - Estimate Capital and Operating Costs of Naphthalene Removal
Massachusetts Institute of Technology

Objective
The objective of this task is to evaluate refinery technologies which can be used to remove naphthalene to determine their feasibility, costs, and effects on fuel composition. This includes calculating the costs of constructing new refinery unit processes and determining additional utility and other operating costs associated with operating the process units responsible for naphthalene removal.

Research Approach
Naphthalene is present in varying levels in the straight-run crude oil distillation cuts used to produce jet fuel. For cuts which exceed the 3% volume limit on naphthalenes (ASTM D1655 2016), this exceedance can be resolved solely through blending, since the average naphthalene content of commercial Jet A is ~1.4% (DLA Energy 2013). Reducing the naphthalene content of jet fuel or eliminating it would therefore require the introduction of additional refinery processing. After reviewing several candidate refining processes in the previous year of this project, we have decided to further explore two in detail: selective hydrotreatment and extractive distillation. These processes are both used in industry for reduction or separation of aromatics and show promise in their ability to reduce and remove naphthalene from jet fuel. Selective hydrotreatment reacts hydrogen with the feedstock and leads to removal of impurities and saturation of aromatics. Extractive distillation allows for the full separation of aromatics from the feedstock via polar solvents. The aromatics stream can then be processed to separate mono-aromatics and naphthalenes, with the former stream being returned to the jet fuel blending pool. These processes were chosen for their low added complexity and energy and because they have a minimal effect on the resultant fuel properties. It is, however, important to note that changes in fuel density, specific energy, fuel sulfur content, hydrogen content, and aromatic content will occur and are considered.

We have developed fundamental process models to estimate effects of fuel constituents and completed a literature search to collect data on process energy requirements, capital costs, and operating costs for both hydro-treatment and extractive distillation. In order to evaluate each candidate process, we leverage existing literature to estimate the utility (process fuel, electricity, hydrogen, etc.) requirements for each process, the effect on the composition of the resulting jet fuel, and the capital costs of new refinery equipment required, including the effects and costs of pre-processing and auxiliary process units that may be required. We then compare processes side-by-side in order to demonstrate the trade-offs associated with naphthalene removal at the refinery.

We consider the hypothetical adoption of a policy whereby jet fuel naphthalene content in the U.S. is reduced by 95% via either hydro-treatment or extractive distillation, at each of the 116 operational U.S. refineries with capacity of greater than 1000 barrels per day (BPD). We calculate costs using a stochastic discounted cash flow model of each refinery. Refinery capital costs are calculated using standard cost curve estimation methods, which relate process unit costs to capacity. Cost curves are used for both the primary naphthalene-removing process units (e.g. extractive distillation column or hydrotreater) as well as auxiliary process units (e.g. steam-methane reformer, CLAUS sulfur recovery unit, pressure-swing hydrogen recovery units, and steam generators). Direct operating costs include maintenance, local taxes, insurance, and supplies, calculated as a percentage of capital costs. Variable operating costs such as process water and chemicals are calculated based on the process unit utility requirements. The stochastic refinery model is used to determine the net present value (NPV) of each naphthalene removal process over its operating lifetime. The NPV can also be used to calculate the cost premium (i.e. cents per gallon) associated with the production of naphthalene-free fuel. Cost estimates are considered from two perspectives: that of the fuel market, and that of society. The market perspective computes cost premiums including all cash flows incurred by fuel producers, thus estimating the expected increase in the market price for naphthalene-free jet fuel. The societal cost estimate is computed from a resource-based perspective, placing it on the same basis as the monetization of potential benefits from improved air quality and potential climate impacts. In this perspective, redistribution of resources, e.g. taxes or loan payments, are disregarded, and the discount rate is assumed to be equivalent to society's long-term cost of capital.

Milestone
The work completed for this task was documented in Deliverable 2-1, provided to the FAA on November 30, 2017.

Major Accomplishments
The resource-based (societal) cost premium and market cost premium estimate distributions for a policy in which all US produced jet fuel has its naphthalene content reduced by 95% (to 0.06 vol%) are shown in **Figure** , with cost data presented in 2016 USD. The mean societal cost premium of hydro-treating is found to be 2.4 cents/liter (95% confidence interval (CI): 2.0–2.7) and of extractive distillation is 1.7 cents/liter (95% CI: 1.5–1.0).

The mean market cost premium of hydro-treating is 3.1 cents/liter (95% CI: 2.4–3.7) and of extractive distillation is 2.1 cents/liter (95% CI: 1.7–2.5). Given the average US Gulf Coast cost of jet fuel in 2016 was $0.33/liter, this represents a 9% and 6% increase in the cost of jet fuel for naphthalene removal via hydro-treatment and extractive distillation, respectively.
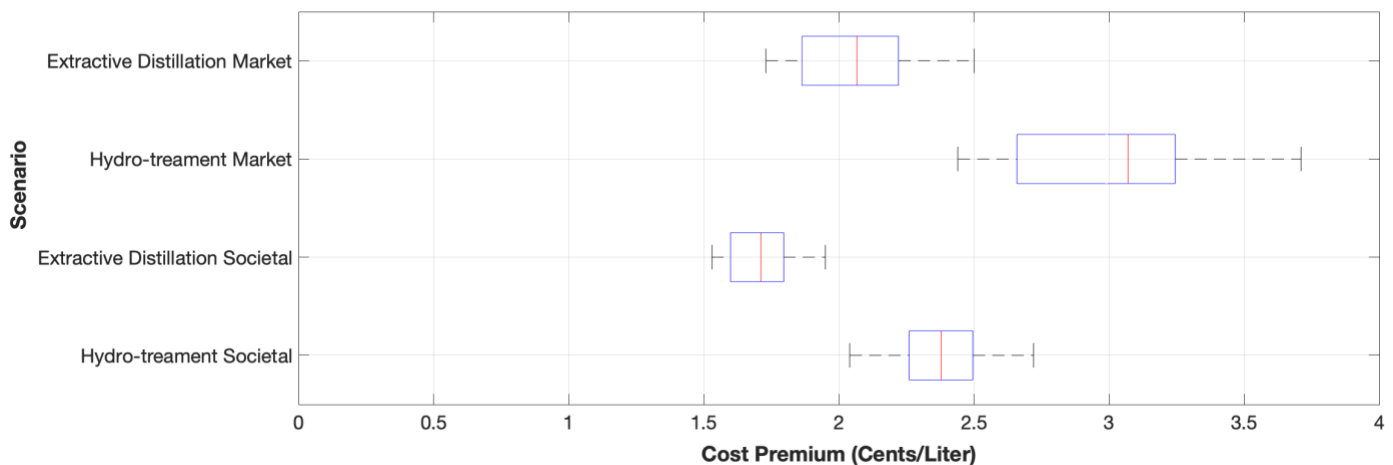

Figure 3: Boxplot for the societal and market cost premiums of hydro-treatment and extractive distillation. All values provided in cents/liter. Red markers represent the distribution means, blue boxes represent the first and third quartiles, and whiskers represent the 95% confidence interval.

Publications
- Weibel, Drew (2018). Techno-economic assessment of jet fuel naphthalene removal to reduce non-volatile particulate matter emissions. S.M. Thesis, Massachusetts Institute of Technology. *https://hdl.handle.net/1721.1/124174*

Outreach Efforts
- ASCENT advisory board presentations (September 2017, April 2018, October 2018)
- Presentation at CRC Aviation Meeting (May 2018) titled "Naphthalene Removal Assessment: Cleaning up Jet Fuel for Reduced Environmental Impacts"
- Presentation at Aviation Emissions Characterization (AEC) Roadmap Annual Meeting (May 2018, May 2020)
- Presentation at the CAEP/12-WG3/2 meeting (October 2019) titled "Economic and Environmental Assessment of Jet Fuel Naphthalene Removal"

Student Involvement
This task was conducted primarily by Drew Weibel, working directly with Prof. Steven Barrett and Dr. Raymond Speth.

References

ASTM. (2016) *D1655: Standard Specification for Aviation Turbine Fuels*. ASTM International.
https://doi.org/10.1520/D1655-16C

DLA Energy. (2013). *Petroleum Quality Information System 2013 Annual Report*. Defense Logistics Agency.

Task 4 - Develop Kinetic Model of PAH formation with fuel-composition effects

Massachusetts Institute of Technology

Objective

The formation of black carbon (soot) from hydrocarbon fuels can be considered as taking place in two stages. First, fuel components and combustion intermediates react to form polycyclic aromatic hydrocarbons (PAHs). Large PAHs then act as soot nuclei, which grow as they absorb both PAH and other species, coagulate through collisions with other soot particles, carbonize, and partially oxidize (Richter and Howard, 2000). The details of fuel composition mainly affect the first step of this process, the formation of PAHs. In this project, we will use the Reaction Mechanism Generator (RMG) to develop a detailed chemical kinetic mechanism for jet fuel combustion that includes the formation of PAH (Gao et al., 2016).

The objective of this task is to update the RMG algorithm in order to handle aromatic species, and to include aromatic reactions up to three-ring species, which will be used as identifiers for soot precursors in later models. The updates to RMG will also undergo preliminary validation using experimental results from shock-tube pyrolysis and co-pyrolysis studies.

Research Approach

Introduction

RMG (http://rmg.mit.edu) is an automatic chemical reaction mechanism generator that constructs kinetic models composed of elementary chemical reaction steps using a general understanding of how molecules react. This tool provides a powerful method to identify reaction mechanisms computationally and ensure full coverage of pertinent species and reactions based on the current literature. RMG has previously been used to analyze various fuels including JP-10 and di-isopropyl ketone combustion and pyrolysis (Gao et al., 2015; Allen et al., 2014).

We will add updates to the RMG algorithm in order to accurately handle aromatic species, and to include aromatic reactions up to three-ring species, which will be used as identifiers for soot precursors in later models.

Method

Previously, RMG was unable to robustly represent aromatic structures. The algorithm depended primarily on representation using Kekulé structures, which resulted in incorrectly treating them like aliphatic species. In order to correctly represent aromatic species, RMG was updated to generate the Clar structure representation of PAHs. As result, aromatic species are more clearly differentiated from aliphatic species, and the number of different representations has been reduced in many cases. An example of the reduced representations for a phenanthrene radical is shown in Figure 4.
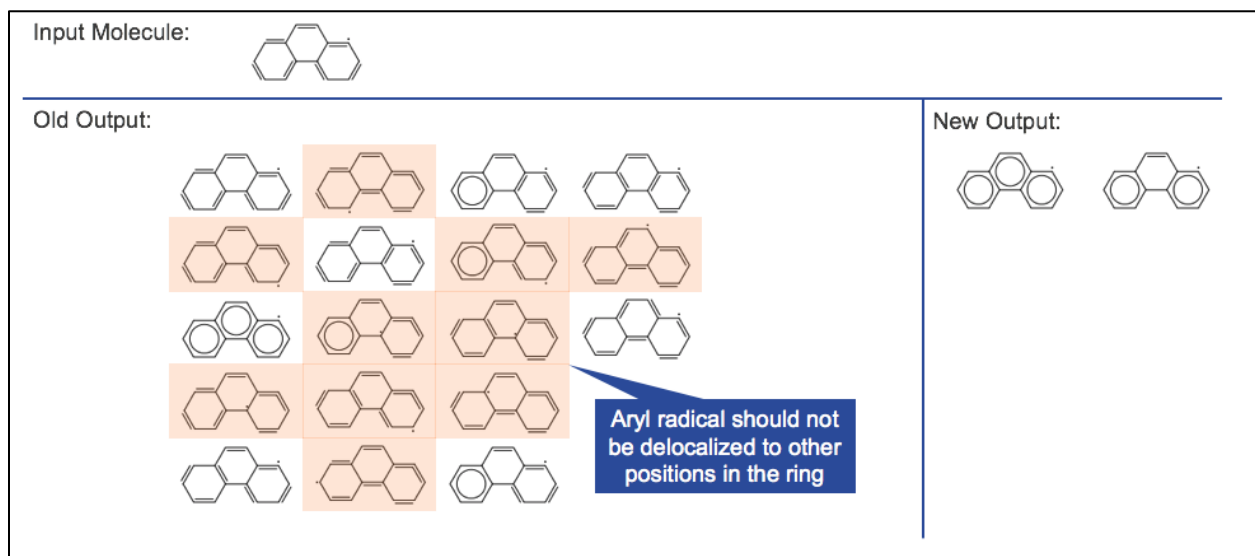
Figure 4: Kekulé and Clar structures for a phenanthrene radical

Other changes were made to further improve reaction rate predictions. An algorithmically challenging task of allowing aromatic bond types was completed after implementing a custom kekulization algorithm. This allows rate rules for aromatic species to be specified separately from those for aliphatic species. Also, ring perception was implemented for rate rules to allow separation of rates for linear versus cyclic species.

In order to validate updates described previously, the RMG model was tested against experimental shock-tube pyrolysis data (Lifshitz et al., 2009). Additional co-pyrolysis models were also generated, although without experimental comparisons.

Results
The improvements described above successfully enabled RMG to handle aromatic species. Prior to the updates, program crashes were inevitable when modeling any aromatic system. To support the algorithm changes, new literature data for aromatic thermochemistry and kinetics were also added to the database.

For preliminary validation, a model was generated for pyrolysis of 1-iodonaphthalene and acetylene for comparison to shock-tube data. The model predictions for the major products, acenaphthalene and naphthalene matched well with the experimental data, as shown in Figure 5. The RMG model predicted a higher yield of 1-ethynyl naphthalene than the literature model, although none was observed in the experiment. The RMG model also predicted smaller side products such as vinylacetylene and 1,3-butadiene, which were not reported in the experiment, although the authors do note that small molecule products from acetylene reactions were assumed to be negligible.

Co-pyrolysis models for equimolar naphthalene or tetralin with acetylene were also generated to get an initial view at whether RMG could capture the differences in reactivity. For naphthalene and acetylene, RMG predicted the major products to be acenaphthalene and hydrogen, which was initially surprising, since other PAHs such as anthracene or phenanthrene were also expected. However, these observations were corroborated by Parker et al. (2015), who also saw that acenaphthalene was the main product in contrast with generally accepted HACA mechanism for PAH growth. The model for tetralin and acetylene displayed markedly different behavior, as expected. Major products were hydrogen, naphthalene, methane, and ethene. No three ring aromatics were formed, possibly because of the overall higher hydrogen/carbon ratio.

Overall, these modeling results are very promising, and show that RMG is now much better at modeling aromatics.

Milestone(s)
This work was completed in June 2017 and is contained in the deliverable 2 presentation provided on Jun 30th, 2017.
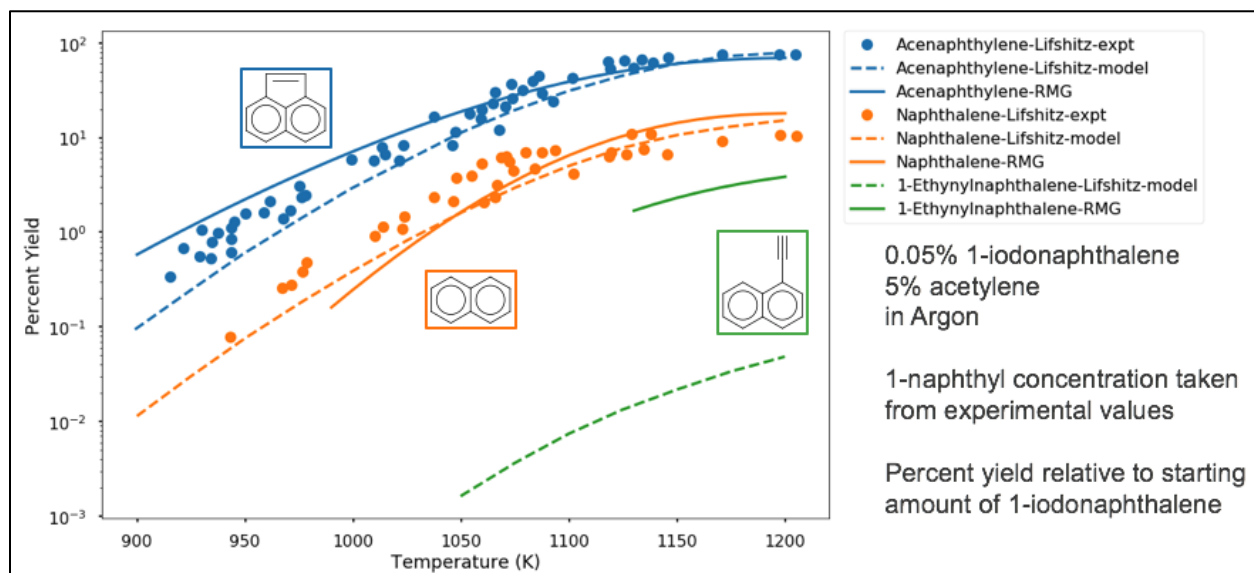
Figure 5: Comparison of yields for selected PAH species in shock tube experiments and kinetic models

Major Accomplishments

During this period, the RMG algorithm was successfully updated to handle aromatic species and kinetics data was added for aromatic species. These updates also underwent preliminary validation when compared to experimental shock-tube pyrolysis data. A summary of this work is contained in the deliverable 2 presentation provided to the FAA on June 30th, 2017.

Publications

- Liu, Mengjie & Green, William H. (2019). Capturing aromaticity in automatic mechanism generation software. Proceedings of the Combustion Institute 37(1), 575–581. *https://doi.org/10.1016/j.proci.2018.06.006*
- Liu, Mengjie (2020). Predictive modeling of polycyclic aromatic hydrocarbon formation during pyrolysis. Ph.D. Thesis, Massachusetts Institute of Technology. *https://hdl.handle.net/1721.1/129925*

Outreach Efforts

- Presentation at the International Conference on Chemical Kinetics (May 2017) titled "Going Bigger: Capturing PAH Chemistry in RMG"
- Presentation at the Aviation Emissions Characterization (AEC) Roadmap Annual Meeting (June 2017)
- Presentation at the 37th International Symposium on Combustion (August 2018) titled "Capturing Aromaticity in Automatic Mechanism Generation Software"

Student Involvement

Mengjie (Max) Liu, PhD student in the Green Research Group in MIT's Department of Chemical Engineering completed the majority of the updates to the RMG and validation and refinement of the RMG models.

References

Allen, J. W., Scheer, A. M., Gao, C. W., Merchant, S. S., Vasu, S. S., Welz, O., Savee, J. D., Osborn, D. L., Lee, C., Vranckx, S., Wang, Z., Qi, F., Fernandes, R. X., Green, W. H., Hadi, M. Z., & Taatjes, C. A. (2014). A coordinated investigation of the combustion chemistry of diisopropyl ketone, a prototype for biofuels produced by endophytic fungi. *Combustion & Flame*, 161(3), 711–724. doi: 10.1016/j.combustflame.2013.10.019

Gao, C. W., Vandeputte, A. G., Yee, N. W., Green, W. H., Bonomi, R. E., Magoon, G. R., Wong, H.-W., Oluwole, O. O., Lewis, D. K., Vandewiele, N. M., & Van Geem, K. M. (2015). JP-10 combustion studied with shock tube experiments and modeled with automatic reaction mechanism generation. *Combustion & Flame* 162(8), 3115–3129. doi: 10.1016/j.combustflame.2015.02.010

Gao C. W., Allen J. W., Green W. H., & West R. H. (2016). Reaction Mechanism Generator: Automatic construction of chemical kinetic mechanisms. *Computer Physics Communications* 203, 212–225. doi: 10.1016/j.cpc.2016.02.013

Lifshitz, A., Tamburu, C., Dubnikova, F. J. (2009). Reactions of 1-Naphthyl Radicals with Acetylene. Single-Pulse Shock Tube Experiments and Quantum Chemical Calculations. Differences and Similarities in the Reaction with Ethylene. *Journal of Physical Chemistry A* 113(39), 10446–10451. doi: 10.1021/jp905448g

Parker, D. S. N., Kaiser, R. I., Bandyopadhyay, B., Kostko, O., Troy, T. P., Ahmed, M. (2015). *Angewandte Chemie* 54(18), 5421–5424. doi: doi.org/10.1002/ange.201411987

Richter, H., & Howard, J. B. (2000). Formation of polycyclic aromatic hydrocarbons and their growth to soot—a review of chemical reaction pathways. *Progress in Energy and Combustion Science* 26(4–6) 565–608. doi: 10.1016/S0360-1285(00)00009-5

Task 5 - Compare kinetic model results to LFP/PIMS experimental data
Massachusetts Institute of Technology

Objective
The growth of aromatic rings as part of PAH formation is controlled by radical reactions, especially the hydrogen abstraction – C_2H_2 addition (HACA) mechanism. The objective of this task is to produce experimental data which can be used to improve estimates of rate coefficients used in chemical kinetic models of PAH formation.

Research Approach
Laser flash-photolysis photoionization mass spectrometry (LFP/PIMS) is an experimental technique in which a photolysis laser pulse initiates controllable, quantifiable radicals in a temperature and pressure controlled reactor. The evolution of the chemical composition in the reactor is then monitored by ionization with VUV light and detection with a mass spectrometer. Experimental conditions are simulated using reactor modeling software, using rate coefficients estimated from the literature. Because these rate coefficients are often pressure dependent, quantum chemistry calculations are used to extrapolate from the low-pressure experimental values to the high pressures relevant to engine operations. Simulations using RMG-generated mechanisms are compared with literature-based rates and the experimental results in order to improve important pathway parameters for aromatic growth.

For this task, two pathways were evaluated. The first is the addition of a vinyl radical (C_2H_3) to acetylene (C_2H_2), which is key step in a formation pathway for benzene (C_6H_6). Studying this system allows us to confirm that we can observe ring formation in our experiment and measure the kinetics and branching ratios which describe C_4H_5/C_4H_4 formation and the yield of benzene, as shown in Figure 6.
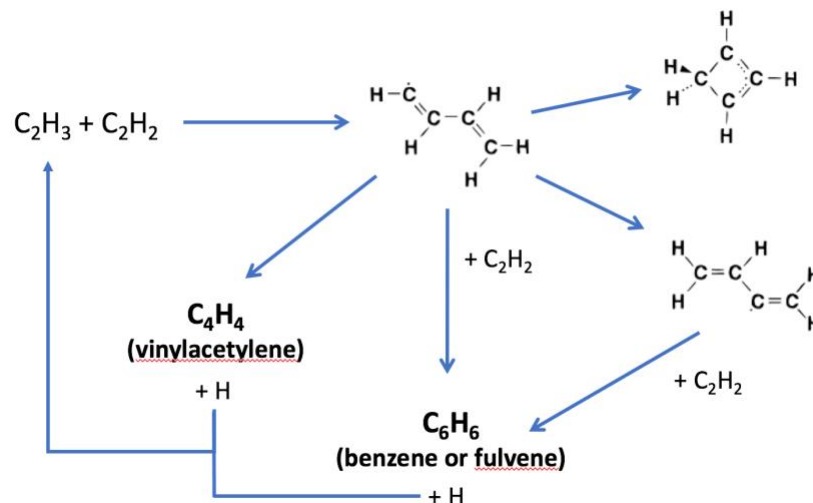

Figure 6: Formation pathways of benzene from vinyl radical and acetylene

The second pathway which was explored is acetylene addition to naphthyl radicals. While aromatic growth from naphthalene is thought to be dominate by the HACA mechanism, under experimental conditions, three-ring PAHs have

generally not been observed. This leads to the question of what other pathways could exist that convert naphthalenes to PAHs, which can be explored using LFP-PIMS.

Milestone
The work completed for this task was documented in Deliverable 2-3, provided to the FAA on April 30, 2018.

Major Accomplishments
Results for the vinyl radical – acetylene pathway, comparing experimental time profiles with simulations, are shown in Figure 7. Kinetics calculated from LFP-PIMS were found to generally agree with the results of the RMG-generated model over a range of temperatures. Preliminary experiments for 1-naphthyl addition to C_2H_2 revealed branching between stable $C_{12}H_8$ products (e.g. acenaphthalene) and $C_{12}H_9$ adducts, as shown in Figure 8. Work is ongoing to incorporate this finding into RMG.
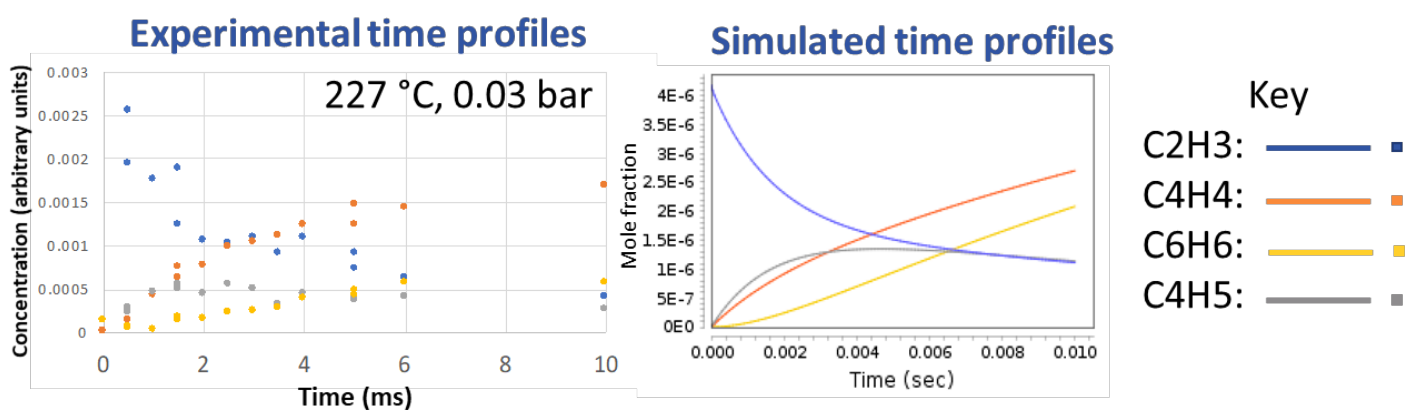

Figure 7: Comparison of experimental and simulated concentration profiles for reaction of vinyl radical and acetylene.
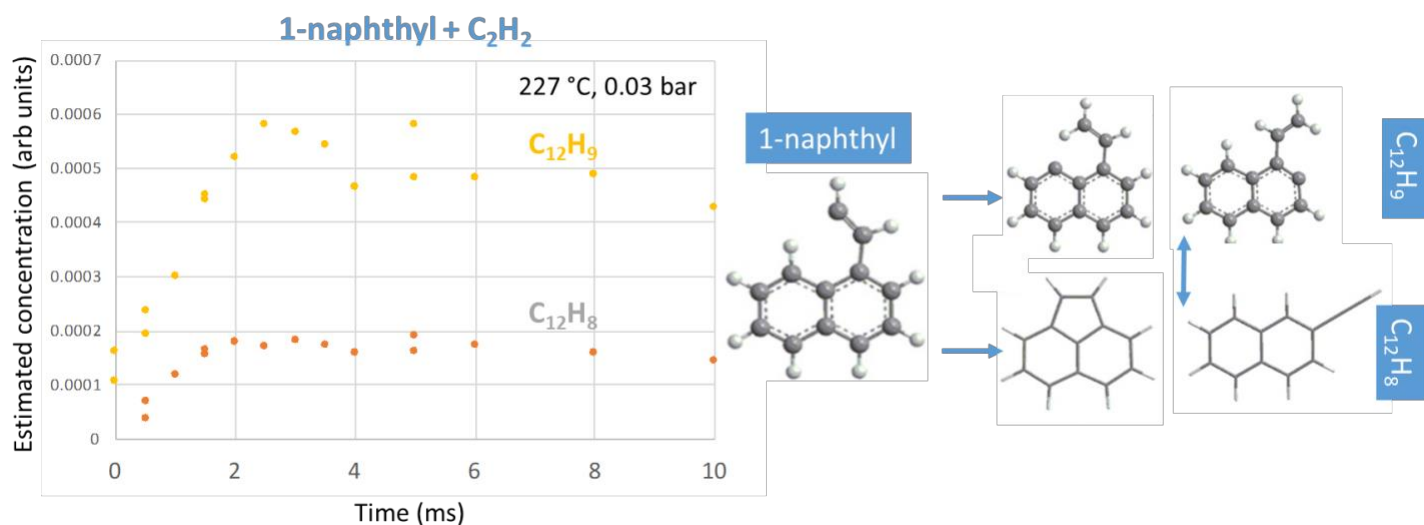

Figure 8: Experimentally-observed branching ratios between stable $C_{12}H_8$ species and $C_{12}H_9$ adducts formed by the reaction of 1-naphthyl radicals with acetylene.

Student Involvement
This work was conducted primarily by Dr. Mica Smith, a postdoctoral associate working under the supervision of Prof. William Green.

Task 6 - Evaluate changes in emissions resulting from removal of naphthalene

Massachusetts Institute of Technology

Objective

Changes to jet fuel composition, such as those achieved by removal of naphthalene using available refining technologies, affect the chemical kinetics of the combustion process in gas turbine engines, which in turn affects the resulting emissions. The formation of black carbon (soot) from hydrocarbon fuels can be considered to take place in two stages. First, fuel components and combustion intermediates react and form PAHs. Large PAHs then act as soot nuclei, which grow as they absorb both PAH and other species, coagulate through collisions with other soot particles, carbonize, and partially oxidize (Richter & Howard, 2000). The details of the fuel composition mainly affect the first step of this process: the formation of PAHs. To enable evaluation of the sensitivity of soot emissions to fuel composition, this task develops a combustor model that includes the detailed chemical kinetic pathways for formation of polycyclic aromatic hydrocarbon (PAH) species from different fuel components and the conversion of these PAH species to soot particles or non-volatile particulate matter (nvPM) emissions. The model also provides the ability to predict changes to CO and NO_x emissions resulting from changes to fuel composition.

Research Approach

The aircraft engine emissions model developed here has three main components: a soot model, an engine model, and a combustor model. The combustor model consists of a reactor network coupled with a gas-phase kinetic mechanism, which is modeled using Cantera (Goodwin et al., 2018). A soot model is added to the reactor network and the interactions between the gas phase and the solid soot phase are modeled in detail. The altitude- and thrust-specific input conditions for the combustor are generated with the engine model. The model is called Pycaso (Python Cantera Soot). The model is used to predict emissions for a CFM56-7B/3 engine because it is one of the most prevalent engines in the commercial fleet, and measurement data for soot emissions from this engine have been published.

Soot model

Due to the uncertainty in soot modeling in gas turbine combustors, a two-equation model is used, which captures all the major soot formation and depletion processes while minimizing complexity. In a two-equation model, the soot number density (N) and mass density (M) are modeled using two equations, which represent the change in soot N and M in response to four soot formation and depletion steps. The standard two-equation model assumes that oxidation solely affects M and does not directly destroy soot particles. However, experiments have shown that oxidation can destroy particles and can thus reduce N (Garo et al., 1988; Lindstedt, 1994). Therefore, an additional term is included in the number density equation to capture the effect of particle destruction through oxidation. It is assumed that for every change in soot mass equivalent to the average soot particle mass, a variable fraction of a particle is destroyed as well. The resulting equations for N and M are

$$\frac{dN}{dt} = C_{\text{nuc}}\left(\frac{dN}{dt}\right)_{\text{nuc}} + C_{\text{coag}}\left(\frac{dN}{dt}\right)_{\text{coag}} + C_{\text{ox},N}\frac{N}{M}C_{\text{ox}}\left(\frac{dM}{dt}\right)_{\text{ox}}, \tag{1}$$

and

$$\frac{dM}{dt} = C_{\text{nuc}}\left(\frac{dM}{dt}\right)_{\text{nuc}} + C_{\text{sg}}\left(\frac{dM}{dt}\right)_{\text{sg}} + C_{\text{ox}}\left(\frac{dM}{dt}\right)_{\text{ox}}. \tag{2}$$

During nucleation, the inception of soot particles happens through collisions of precursor species (Blanquart & Pitsch, 2009). These precursor species are considered to primarily consist of heavy PAH molecules (Dobbins et al., 1998; Schuetz & Frenklach, 2002). When two PAH molecules collide and stick together, they form a PAH dimer, which again increases in size through collisions with other PAH species and dimers. This growth through collisions allows for transitioning from the gas phase to the solid phase and results in the first solid incipient soot particle (Martini, 2008). PAH-PAH collision rates are considered for nucleation in the model, while PAH-soot collisions are modeled as surface growth. The nucleation rate resulting from collisions of PAH species i and j is based on the collision frequency $\beta_{i,j}$ and is given by

$$\left(\frac{dN}{dt}\right)_{\text{nuc},ij} = \frac{\gamma_i + \gamma_j}{2}\varepsilon\sqrt{\frac{8\pi k_B T}{\mu_{i,j}}}N_A^2(r_i + r_j)^2[\text{PAH}_i][\text{PAH}_j], \tag{3}$$

where $\varepsilon = 2.2$ is the Van der Waals enhancement factor, k_B is the Boltzmann constant, N_A is Avogadro's constant, r_i and r_j are the radii of PAH species i and j, $\mu_{i,j}$ is the reduced mass of PAH species i and j and $[\mathrm{PAH}_i]$ is the concentration of PAH species i (An et al., 2016; Atkins et al., 2018; Blanquart & Pitsch, 2009). The sticking coefficient $\gamma < 1$ is computed using the assumption that it scales with PAH mass to the fourth power (Blanquart & Pitsch, 2009). The PAH species are chosen such that no direct pathways from species in the fuel surrogates to soot mass through nucleation exist, as these pathways might result in an overestimation of sensitivities to fuel composition. The total nucleation rate is calculated by taking the sum over all the PAH species in the gas-phase mechanism.

Nucleation is followed by surface growth and coagulation. During surface growth, the soot particles grow in size and mass due to the adsorption of gas phase molecules, mainly acetylene (Omidvarborna et al., 2015). Growth rates are found to be much higher than nucleation rates and most of the soot mass is thought to form during this step in the process (Martini, 2008). Here, two types of surface growth mechanisms are implemented. The first assumes surface growth solely by acetylene, whereas the second also includes surface growth through condensation of PAH species on the soot surface. In order to include surface growth through the adsorption of PAH species, the surface growth source term is expanded with an additional term. This term is based on the collision frequency of soot particles with PAH species i and is given by

$$\left(\frac{dM}{dt}\right)_{\mathrm{sg,PAH}} = \sum_{i=1}^{L} n_{\mathrm{C},i} W_{\mathrm{C}} \frac{\gamma_i + \gamma_{soot}}{2} \varepsilon \sqrt{\frac{8\pi k_B T}{\mu_{\mathrm{soot},i}}} \left(r_i + \frac{d_p}{2}\right)^2 [\mathrm{PAH}_i] N. \tag{4}$$

Since this term is similar to the nucleation term, it is scaled with C_{nuc} instead of C_{sg}.

During coagulation, soot particles grow further in size through particle-particle collisions (Blanquart & Pitsch, 2009; Omidvarborna et al., 2015). The total number of soot particles decreases during coagulation whereas the total mass across all particles stays constant. The implemented coagulation mechanism is based on the collision of two spherical particles with a collision rate as defined by Puri et al. (1993). The resulting source term for the number density equation is given by

$$\left(\frac{dN}{dt}\right)_{\mathrm{coag}} = -K_{\mathrm{coag}} \sqrt{\frac{24 R_u T}{\rho_{\mathrm{soot}} N_A}} \sqrt{d_p} N^2, \tag{5}$$

where ρ_{soot} is assumed to be equal to 2000 kg/m³ and K_{coag} is a constant ranging between 1 and 9 in literature (Brookes & Moss, 1999; Wen et al., 2003).

In contrast to the previous three steps, soot is destroyed during oxidation. Oxidation significantly reduces the amount of soot and measurements suggest that most of the soot formed at the start of the combustion process is oxidized before reaching the combustor exit (Toone, 1968). Carbon and hydrogen atoms are removed from the soot agglomerates by reactions with primarily diatomic oxygen (O_2), hydroxyl radicals (OH) and atomic oxygen (O) (Louloudi, 2003; Neoh et al., 1981). Their respective contributions to the oxidation source term (Guo et al., 2016; Martini, 2008; Schiener & Lindstedt, 2018) are given by

$$\left(\frac{dM}{dt}\right)_{\mathrm{ox},O_2} = -745.88 \eta_{O_2} W_{\mathrm{C}} \sqrt{T} \exp\left(-\frac{19{,}680}{T}\right) [O_2] A_s, \tag{6}$$

and

$$\left(\frac{dM}{dt}\right)_{\mathrm{ox,OH}} = -\eta_{\mathrm{OH}} W_{\mathrm{C}} \sqrt{T} [\mathrm{OH}] A_s, \tag{7}$$

and

$$\left(\frac{dM}{dt}\right)_{\mathrm{ox,O}} = -1.82 \eta_O W_{\mathrm{C}} \sqrt{T} [O] A_s, \tag{8}$$

where the collision efficiencies for O_2 and O (η_{O_2} and η_O) are assumed to be unity (Mueller et al., 2009; Wen et al., 2003). For oxidation through OH, collision efficiency values ranging from 0.01 to 0.65 have been proposed (Fenimore & Jones,

1967; Ghiassi et al., 2017; Guo et al., 2016; Haudiquert et al., 1997; Neoh et al., 1981; Puri et al., 1994; Richter et al., 2005; Schiener & Lindstedt, 2018). We use a value of 0.13, determined by Neoh et al. (1981), as baseline value in this model.

Engine model

The combustor inlet temperature (T_3) and pressure (P_3), as well as the mass flows of fuel ($\dot{m}_{fuel}$) and air ($\dot{m}_{air}$) entering the combustor are computed using a detailed engine model of the CFM56-7B engine. The engine model is developed using the Numerical Propulsion System Software (NPSS) and matches fuel flows, thrust levels and pressure ratios from the ICAO engine emissions databank (EDB) within 5%. The temperature of the gas-phase mixture entering the combustor is corrected for vaporization of the fuel by adjusting the specific enthalpy of the gas-fuel mixture as follows

$$h_{mix} = \frac{1}{\dot{m}_{air}} \left[\dot{m}_{air} h_{air, P_3 T_3} + \dot{m}_{fuel} h_{fuel, P_3 T_3} - \dot{m}_{fuel}(L + \Delta h) \right], \tag{9}$$

where L represents the enthalpy of vaporization at standard conditions (T =298.15 K and P = 101,325 Pa), h is the specific enthalpy and Δh is the change in specific enthalpy going from standard conditions to T_3 and P_3. $\dot{m}_{fuel}$ and $\dot{m}_{air}$ are the mass flow rates of fuel and air, respectively.

Combustor model

The combustor model developed for this project represents a Rich-Burn Quick-Mix Lean-Burn (RQL) combustor. Figure 9 shows a schematic overview of the model. The model is divided into two parts: the primary zone and the secondary zone. In the primary zone, air and fuel are mixed at a certain equivalence ratio. Then, the quenching happens at the start of the secondary zone through to the addition of secondary air in the slow and fast mixing zones. In the second part of the secondary zone, dilution air is added to represent the lean burn zone. As NO_x, CO and soot reactions are found to be quenched at the end of the secondary zone, the turbine is not modeled. The gas phase chemistry inside the combustor model is modeled using a kinetic mechanism which determines the structure of the flame and specifies the species profile (Appel et al., 2000). A high temperature kinetic mechanism for transportation fuels is coupled with a NO_x mechanism, resulting in a chemical mechanism consisting of 218 species and 7047 reactions (Ranzi et al., 2012, 2014, 2015).

The combustor model can be used to represent different (RQL) combustors. In order to represent a specific combustor design, combustor model parameters are calibrated using emissions data from the EDB for an engine containing that specific combustor. Since the combustor model can be considered a "black box" function and obtaining a (numerical) gradient is computationally expensive, gradient-free optimization is used to calibrate the model parameters. More specifically, the DIvided RECTangles (DIRECT) method is applied (Finkel, 2003; Hicken et al., 2012; Jones, 2009).

Milestone

The combined combustor, soot, and engine model described above were implemented, and used to explore the impact of different jet fuel compositions on NO_x, CO, and soot emissions.

Major Accomplishments

Model validation

Eight different soot model configurations (C1 – C8) were developed. Each configuration consists of a different set of reaction rate coefficients and/or soot mechanisms. These eight configurations are selected in order to capture a range of soot mechanisms in literature and to quantify the impact and behavior of each step of the soot formation process. The performance of the configurations against measurements for both EI mass and number is summarized in Figure 10. Starting with EI soot mass, two clusters of configurations are visible. Configurations 1-5 capture the trends in the validation data for thrust levels >= 30%. On the other hand, configurations 6-8 capture the trend in the data for thrust settings larger than approximately 75% but underpredict soot mass emissions thrust settings lower than 75%. For soot number EI, the models all capture the trend in the validation data of decreasing number EI with increasing thrust between approximately 60% and 100% thrust. Configurations 4,5 and 6 also capture the 30% thrust point, whereas configurations 1,2,7 and 8 underpredict soot number at this thrust setting, while configuration 3 overpredicts it.
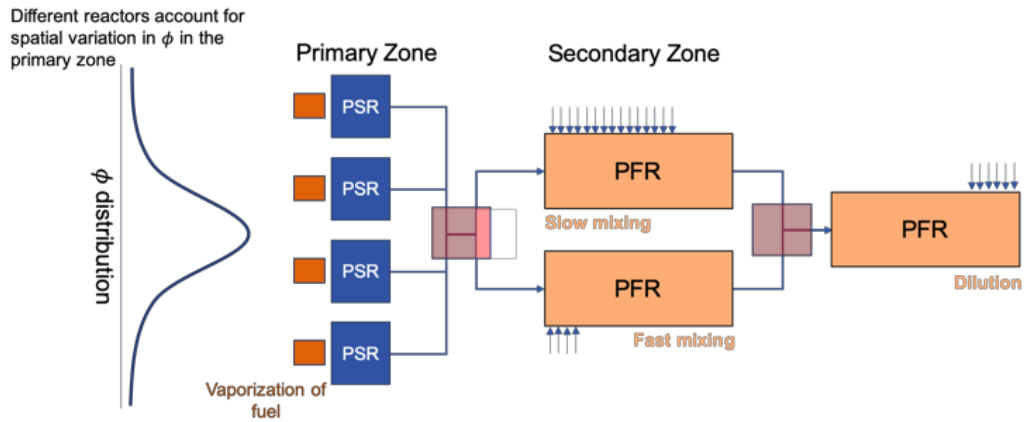
Figure 9. Schematic overview of the combustor model. Multiple well-stirred reactors (WSR) are used in the primary zone. The secondary zone uses a combination of plug flow reactors (PFR) to simulate different mixing times. The arrows represent secondary and dilution air entering the combustor.

We find that primary zone soot mass formation peaks at $\varphi \approx 2.3$, where the EI soot is approximately 7 times higher than at $\varphi \approx 3.0$ and $\varphi \approx 2.0$. On the other hand, soot number increases with equivalence ratio and peak EI soot number values are observed in the richest reactors. This difference is explained by the PAH concentration being the limiting factor for nucleation (soot number), whereas temperature and C_2H_2 concentration are the limiting factors for soot mass (surface growth).

In order to validate the model's capability to predict changes in soot emissions in response to changing fuel compositions, we simulate a subset of the experiments conducted by Brem et al. (2015) where soot emissions are measured for two fuel blends with different naphthalene and aromatic content. The soot predictions of each of the model configurations for two versions of each of the 5 surrogates are evaluated. The total aromatics % v/v, naphthalene % v/v and hydrogen content of these two fuels match the values used in experiments by Brem et al. (2015). The resulting changes in EI soot mass and
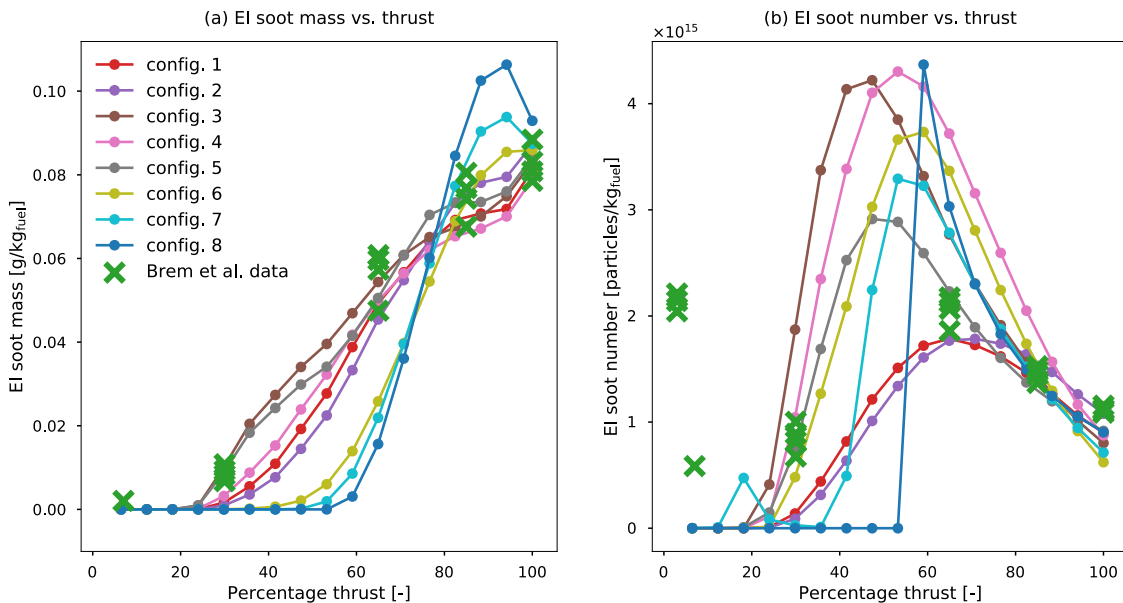

Figure 10. Comparison of EI soot (a) mass and (b) number with validation data (surrogate 4).
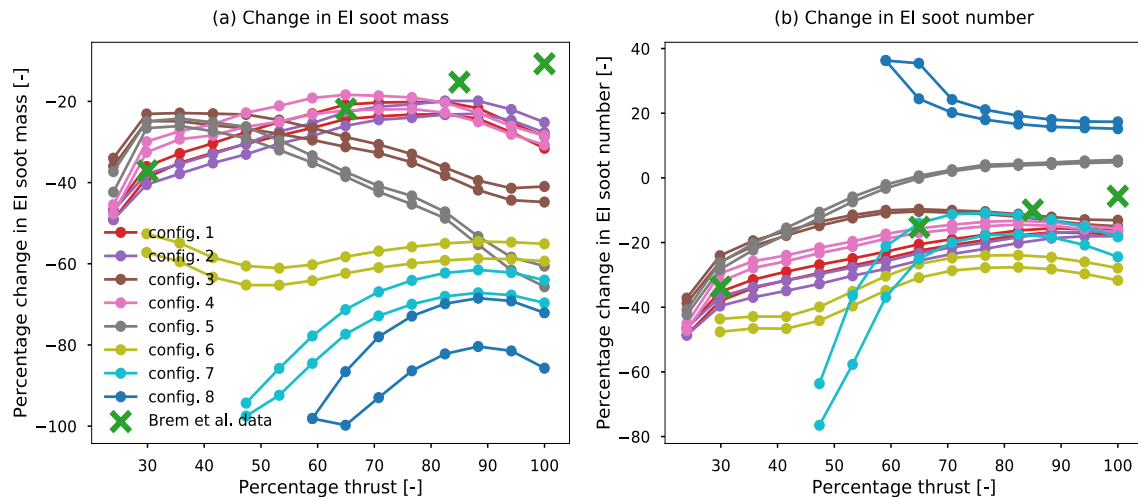
Figure 11. Comparison of model predictions with experimental data by Brem et al. (2015). Percentage change in EI soot (a) mass and (b) number for all eight configurations.

number are shown in Figure 11. We see that the three configurations using the hydrogen abstraction acetylene addition (HACA) mechanisms show large discrepancies for both soot mass and number. The five other configurations can be grouped based on their values for C_{coag} and $C_{\text{ox},N}$. The three configurations (1,2 and 4) with relatively low coagulation factors (<30) and relatively large $C_{\text{ox},N}$ values (> 0.65) match the soot mass data from Brem et al. (2015) within 5 percentage points (p.p.) at 30% and 65% thrust, 8 p.p. at 85% thrust and 18 p.p. at 100% thrust, and within 15 p.p. of the soot number data for all thrust conditions. When increasing the coagulation factor and decreasing $C_{\text{ox},N}$ (configurations 3 and 5) these differences grow to a maximum of 51 p.p. at 100% thrust for configuration 5. A possible explanation for the relatively large discrepancies at high thrust for the configuration using high coagulation factors is that these configurations rely on a large N in the PZ to increase the average particle size (and thus the M/A_s ratio). When reducing the naphthalene content of the fuel, less nucleation occurs and the soot number density decreases. This again reduces coagulation and increases M/A_s which leads to more oxidation in the secondary zone. On the other hand, configurations relying on $C_{\text{ox},N}$ to reduce N, are not affected as much by a decreasing N. Due to their superior performance compared on the validation data, configurations 1,2 and 4 are selected to assess the sensitivity of soot to naphthalene removal and biofuels in the subsequent analysis of fuel composition effects.

Effects of fuel composition
Figure 12 shows the computed ranges of soot mass and number emissions reductions associated with the naphthalene removal through extractive distillation and hydrotreating. These ranges represent both variations in the three soot model configurations as well as the five baseline fuel compositions. The mean reductions in EI mass are approximately 20 p.p. higher for extractive distillation than for hydrotreating. For EI soot number, the differences between the means of the two methods range from 12 p.p. at 100% thrust to 28 p.p. at 30% thrust. These differences are explained by tetralin, the product of hydrotreating naphthalene, still being an aromatic species and having a relatively short pathway to becoming a PAH species during combustion. Reductions in mass are predicted to be larger than reductions in number (for >35% thrust), which is consistent with literature (Brem et al., 2015; Speth et al., 2015).
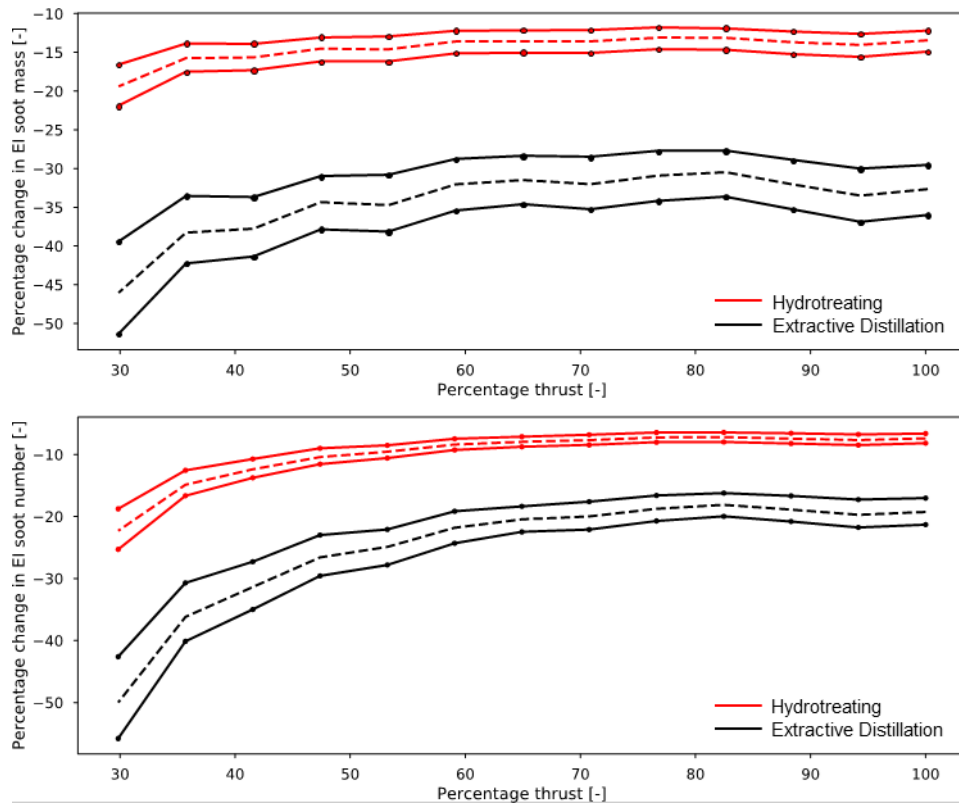
Figure 12. Ranges of predicted effects of naphthalene removal from jet fuel by hydrotreating (red) and extractive distillation (black) on EI soot (a) mass and (b) number emissions indices. The dashed lines represent the means of the prediction ranges, which capture variations in three different soot configurations and five different surrogates.

Furthermore, especially for number emissions, reductions increase with decreasing thrust. This effect is also observed in experiments in literature (Brem et al., 2015; Corporan et al., 2007; Naegeli & Moses, 2015; Speth et al., 2015). We find that the increasing change in soot emissions with decreasing thrust is explained by two main factors. The first one is that sensitivity to fuel composition increases with decreasing PZ equivalence ratio. The changes in EI soot mass and number due to naphthalene removal are found to be approximately 1.5 and 2-3 times higher at φ=2.2 compared to φ=3.0, respectively. The lower the thrust setting, the lower the primary zone equivalence ratio(s), and thus the higher the sensitivity to fuel composition. The second factor is that for a given φ, the reductions in both soot mass and number increase with decreasing thrust. This is explained by the temperature difference between the thrust conditions. Higher temperatures at higher thrust settings make the reactor more resilient to changes in naphthalene concentrations.

Figure 13 shows the predicted effects of using 20%, 50% and 100% biofuel blends on soot emissions. As expected, mean reductions increase with increasing the biofuel fraction and decreasing thrust. The predicted reductions for soot mass range from 17%, 37% and 55% at 100% thrust to 25%, 56% and 92% at 30% thrust. For soot number, mean reductions at 100% thrust are 11%, 26% and 51% compared to reductions of 24%, 56% and 92% at 30% thrust.

The effect of using 20%, 50% and 100% biofuel blends on NO$_x$ and CO emissions is shown in Figure 14. The model predicts mean reductions in NO$_x$ emissions of 2%, 5% and 10% and reductions in CO emissions of 1%, 2% and 5% for the three blends, respectively. The sharp drop in CO at the lowest thrust setting is a consequence of the finite number of reactors in the model and the corresponding CO values are therefore not considered. This sharp drop in CO occurs because the leanest reactor blows out for the standard surrogate and does not for the 50% and 100% biofuel blends. This leads to an increase in SZ mixing temperature and thus CO depletion.
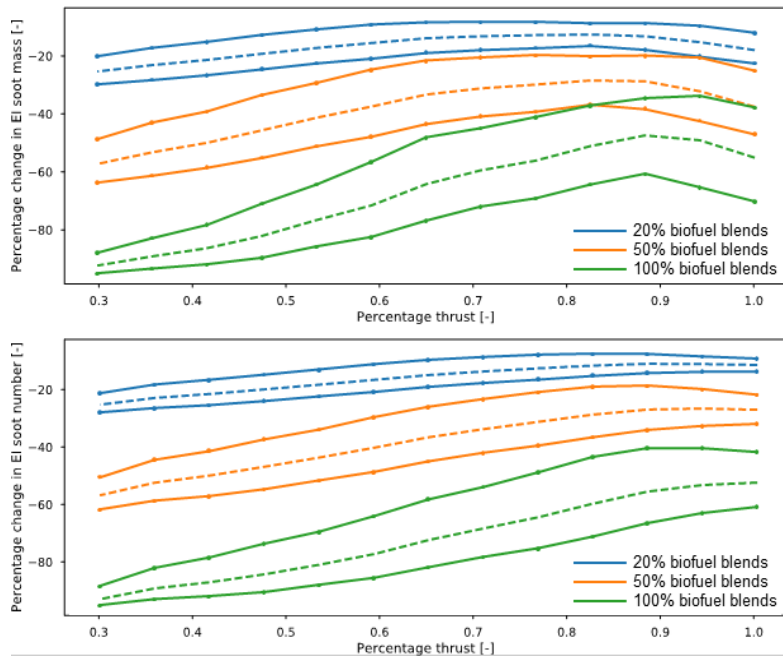
Figure 13. Effects of using 20% (blue), 50% (orange) and 50% (green) biofuel blends on EI soot (a) mass and (b) number. The dashed lines represent the means of the prediction ranges, which capture variations in three different soot mechanisms and five different surrogates.
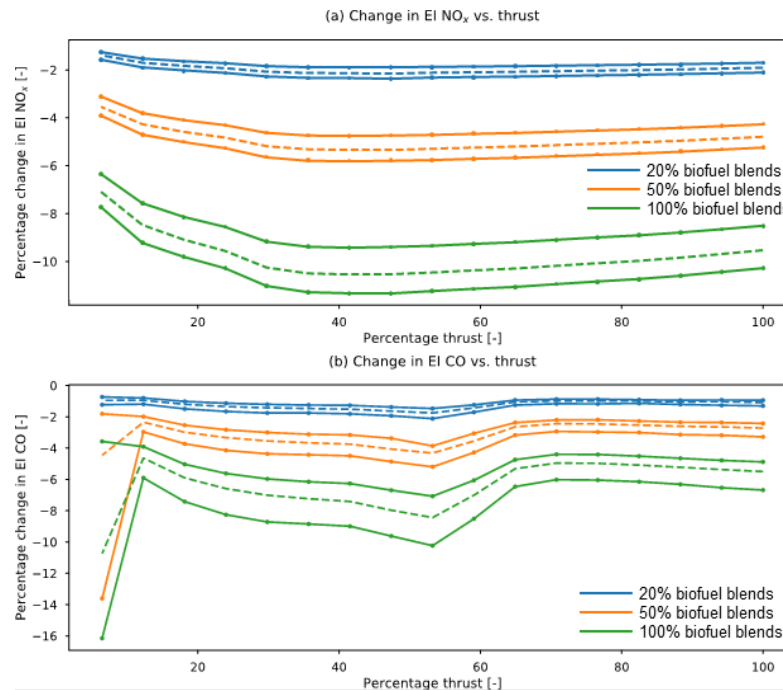

Figure 14. Effects of using 20% (blue), 50% (orange) and 100% (green) biofuel blends on (a) NO$_x$ and (b) CO emissions. The dashed lines represent the means of the prediction ranges, which capture variations in five different surrogates.

Publications

- Brink, Lukas (2020). Modeling the impact of fuel composition on aircraft engine NO_x, CO and soot emissions. S.M. Thesis, Massachusetts Institute of Technology. *https://hdl.handle.net/1721.1/129181*

Outreach Efforts

- ASCENT advisory board presentations (October 2018, October 2019, March 2020)
- Presentations at the Aviation Emissions Characterization (AEC) Roadmap Annual Meeting (June 2017, May 2020)

Student Involvement

This task was conducted primarily by Lukas Brink, working directly with Prof. Steven Barrett and Dr. Raymond Speth. Mr. Brink graduated with a Master of Science in 2020.

References

An, Y., Li, X., Teng, S., Wang, K., Pei, Y., Qin, J., & Zhao, H. (2016). Development of a soot particle model with PAHs as precursors through simulations and experiments. *Fuel*, *179*, 246–257. https://doi.org/10.1016/j.fuel.2016.03.100

Appel, J., Bockhorn, H., & Frenklach, M. (2000). Kinetic modeling of soot formation with detailed chemistry and physics: Laminar premixed flames of C_2 hydrocarbons. *Combustion and Flame*, *121*(1–2), 122–136.

Atkins, P. W., De Paula, J., & Keeler, J. (2018). *Atkins' physical chemistry*. Oxford University Press.

Blanquart, G., & Pitsch, H. (2009). A joint volume-surface-hydrogen multi-variate model for soot formation. *Combustion Generated Gine Carbonaceous Particles*, 437–463.

Brem, B.T., Durdina, L., Siegerist, F., Beyerle, P., Bruderer, K., Rindlisbacher, T., Rocci-Denis, S., Andac, M.G., Zelina, J., Penanhoat, O., & Wang, J. (2015). Effects of fuel aromatic content on nonvolatile particulate emissions of an in-production aircraft gas turbine. Environmental Science & Technology, 49 13149–57

Brookes, S. J., & Moss, J. B. (1999). Predictions of soot and thermal radiation properties in confined turbulent jet diffusion flames. *Combustion and Flame*, *116*(4), 486–503. https://doi.org/10.1016/S0010-2180(98)00056-X

Corporan, E., DeWitt, M. J., Belovich, V., Pawlik, R., Lynch, A. C., Gord, J. R., & Meyer, T. R. (2007). Emissions Characteristics of a Turbine Engine and Research Combustor Burning a Fischer–Tropsch Jet Fuel. *Energy & Fuels*, *21*(5), 2615–2626. https://doi.org/10.1021/ef070015j

Dobbins, R. A., Fletcher, R. A., & Chang, H.-C. (1998). The evolution of soot precursor particles in a diffusion flame. *Combustion and Flame*, *115*(3), 285–298. https://doi.org/10.1016/S0010-2180(98)00010-8

Fenimore, C. P., & Jones, G. W. (1967). Oxidation of soot by hydroxyl radicals. *The Journal of Physical Chemistry*, *71*(3), 593–597. https://doi.org/10.1021/j100862a021

Finkel, D. (2003). *DIRECT optimization algorithm user guide*. North Carolina State University. Center for Research in Scientific Computation.

Garo, A., Lahaye, J., & Prado, G. (1988). Mechanisms of formation and destruction of soot particles in a laminar methane-air diffusion flame. *Symposium (International) on Combustion*, *21*(1), 1023–1031. https://doi.org/10.1016/S0082-0784(88)80333-3

Ghiassi, H., Lignell, D., & Lighty, J. S. (2017). Soot Oxidation by OH: Theory Development, Model, and Experimental Validation. *Energy & Fuels*, *31*(3), 2236–2245. https://doi.org/10.1021/acs.energyfuels.6b02193

Goodwin, D. G., Speth, R. L., Moffat, H. K., & Weber, B. W. (2018). *Cantera: An object-oriented software toolkit for chemical kinetics, thermodynamics, and transport processes*. Version 2.4.0. https://www.cantera.org.

Guo, H., Anderson, P. M., & Sunderland, P. B. (2016). Optimized rate expressions for soot oxidation by OH and O2. *Fuel*, *172*, 248–252. https://doi.org/10.1016/j.fuel.2016.01.030

Haudiquert, M., Cessou, A., Stepowski, D., & Coppalle, A. (1997). OH and soot concentration measurements in a high-temperature laminar diffusion flame. *Combustion and Flame*, *111*(4), 338–349. https://doi.org/10.1016/S0010-2180(97)00003-5

Hicken, J., Alonso, J., & Farhat, C. (2012). *Introduction to multidisciplinary design optimization: Chapter 6: Gradient-free optimization*. Stanford University.

Jones, D. R. (2009). Direct global optimization algorithm. *Encyclopedia of Optimization*, *1*(1), 431–440.

Lindstedt, P. R. (1994). Simplified Soot Nucleation and Surface Growth Steps for Non-Premixed Flames. In H. Bockhorn (Ed.), *Soot Formation in Combustion: Mechanisms and Models* (pp. 417–441). Springer. https://doi.org/10.1007/978-3-642-85167-4_24

Louloudi, S. (2003). *Transported probability density function: Modelling of turbulent jet flames*. Imperial College London (University of London).

Martini, B. (2008). *Development and assessment of a soot emissions model for aircraft gas turbine engines* [Thesis, Massachusetts Institute of Technology]. https://dspace.mit.edu/handle/1721.1/45256

Mueller, M. E., Blanquart, G., & Pitsch, H. (2009). Hybrid Method of Moments for modeling soot formation and growth. *Combustion and Flame*, *156*(6), 1143–1155. https://doi.org/10.1016/j.combustflame.2009.01.025

Naegeli, D. W., & Moses, C. A. (2015, April 17). *Effect of Fuel Molecular Structure on Soot Formation in Gas Turbine Engines*. ASME 1980 International Gas Turbine Conference and Products Show. https://doi.org/10.1115/80-GT-62

Neoh, K. G., Howard, J. B., & Sarofim, A. F. (1981). Soot Oxidation in Flames. In D. C. Siegla & G. W. Smith (Eds.), *Particulate Carbon: Formation During Combustion* (pp. 261–282). Springer US. https://doi.org/10.1007/978-1-4757-6137-5_9

Omidvarborna, H., Kumar, A., & Kim, D.-S. (2015). Recent studies on soot modeling for diesel combustion. *Renewable and Sustainable Energy Reviews*, *48*, 635–647. https://doi.org/10.1016/j.rser.2015.04.019

Puri, R., Richardson, T. F., Santoro, R. J., & Dobbins, R. A. (1993). Aerosol dynamic processes of soot aggregates in a laminar ethene diffusion flame. *Combustion and Flame*, *92*(3), 320–333.

Puri, R., Santoro, R. J., & Smyth, K. C. (1994). *Oxidation of Soot and Carbon Monoxide in Hydrocarbon Diffusion Flames*. *97*, 125–144.

Ranzi, E., Cavallotti, C., Cuoci, A., Frassoldati, A., Pelucchi, M., & Faravelli, T. (2015). New reaction classes in the kinetic modeling of low temperature oxidation of n-alkanes. *Combustion and Flame*, *162*(5), 1679–1691. https://doi.org/10.1016/j.combustflame.2014.11.030

Ranzi, E., Frassoldati, A., Grana, R., Cuoci, A., Faravelli, T., Kelley, A. P., & Law, C. K. (2012). Hierarchical and comparative kinetic modeling of laminar flame speeds of hydrocarbon and oxygenated fuels. *Progress in Energy and Combustion Science*, *38*(4), 468–501. https://doi.org/10.1016/j.pecs.2012.03.004

Ranzi, E., Frassoldati, A., Stagni, A., Pelucchi, M., Cuoci, A., & Faravelli, T. (2014). Reduced Kinetic Schemes of Complex Reaction Systems: Fossil and Biomass-Derived Transportation Fuels. *International Journal of Chemical Kinetics*, *46*(9), 512–542. https://doi.org/10.1002/kin.20867

Richter, H., Granata, S., Green, W. H., & Howard, J. B. (2005). Detailed modeling of PAH and soot formation in a laminar premixed benzene/oxygen/argon low-pressure flame. *Proceedings of the Combustion Institute*, *30*(1), 1397–1405. https://doi.org/10.1016/j.proci.2004.08.088

Schiener, M. A., & Lindstedt, R. P. (2018). Joint-scalar transported PDF modelling of soot in a turbulent non-premixed natural gas flame. *Combustion Theory and Modelling*, *22*(6), 1134–1175. https://doi.org/10.1080/13647830.2018.1472391

Schuetz, C. A., & Frenklach, M. (2002). Nucleation of soot: Molecular dynamics simulations of pyrene dimerization. *Proceedings of the Combustion Institute*, *29*(2), 2307–2314. https://doi.org/10.1016/S1540-7489(02)80281-4

Speth, R. L., Rojo, C., Malina, R., & Barrett, S. R. H. (2015). Black carbon emissions reductions from combustion of alternative jet fuels. *Atmospheric Environment*, *105*, 37–42. https://doi.org/10.1016/j.atmosenv.2015.01.040

Toone, B. (1968). A Review of Aero Engine Smoke Emission. In I. E. Smith (Ed.), *Combustion in Advanced Gas Turbine Systems* (pp. 271–296). Pergamon. https://doi.org/10.1016/B978-0-08-013275-4.50019-2

Wen, Z., Yun, S., Thomson, M. J., & Lightstone, M. F. (2003). Modeling soot formation in turbulent kerosene/air jet diffusion flames. *Combustion and Flame*, *135*(3), 323–340. https://doi.org/10.1016/S0010-2180(03)00179-2

Task 7 - Calculate Air Quality and Climate Impacts of Naphthalene Removal

Massachusetts Institute of Technology

Objective

The objective of this task is to calculate the air quality and climate impacts of a policy in which naphthalene is removed from jet fuel used in the United States.

Research Approach

The air quality effects of changes in aircraft PM emissions are evaluated by using the GEOS-Chem adjoint model, which we have previously used for assessing health impacts of emissions (Dedoussi & Barrett, 2014). The use of an adjoint model, which is a computationally efficient approach to calculating the sensitivity of an aggregate objective function (e.g., population exposure to $PM_{2.5}$), enables evaluation of a range of scenarios in a single run, thus allowing for incorporation of upstream uncertainty in the emissions indices for different species. The PM exposure calculated by using GEOS-Chem includes both the effects of changes in black carbon emissions and changes due to sulfur reductions that accompany the removal of naphthalenes (in the case in which hydrotreating is used to remove naphthalenes). The spatial pattern of emissions of nvPM, and sulfur compounds is taken from the 2015 inventory from the Aviation Environmental Design Tool (AEDT).

Climate impacts of naphthalene removal include contributions at both the fuel production and fuel consumption stages.

The additional refinery processing required to reduce or remove naphthalene requires process fuel, steam, electricity, and, in the case of hydrotreating, hydrogen production. The greenhouse gas (GHG) emissions associated with each of these processes increase life-cycle jet fuel GHG emissions. Using the results calculated as part of the refinery modeling work conducted in the previous project year, we found the GHG emissions associated with naphthalene removal to be 135 g CO_2e per kg fuel for hydrotreating and 144 g CO_2e per kg fuel for extractive distillation.

Consumption of reduced-naphthalene fuel decreases radiative forcing (RF) from aviation black carbon, and reductions in sulfur decrease the cooling effect of sulfates (Mahashabde et al., 2011). Contrail impacts are estimated according to studies on the impact of reducing the number of ice nuclei available for contrail formation. Caiazzo et al. (2017) have found that decreasing ice nuclei by 67% (an amount representative of a fully paraffinic biofuel) reduces contrail RF by <13%. Burkhardt et al. (2018) found that reducing ice nuclei by 50% reduces contrail RF by ~20%. Here, the reductions in contrail RF found in these studies are scaled by the estimated reduction in nvPM emissions from naphthalene removal.

The combined climate impacts of these effects are evaluated by using the APMT-Impacts Climate model, a policy-oriented rapid assessment tool that provides probabilistic estimates of climate impacts.

Milestone
The work completed for this task was documented in Deliverable 2-4, provided to the FAA on May 31, 2018.

Major Accomplishments
On the basis of a literature review of nvPM emissions measurements from engines using fuels with varying levels of naphthalene (Brem et al., 2015; DeWitt et al., 2008), the potential range of reduction in nvPM emissions associated with 95% naphthalene removal was estimated to be 15–40%, or 5.0–12.5 mg nvPM per kg fuel. Monetized climate impacts for the different climate forcing pathways are summarized in Table 2, presented on a cents-per-gallon basis with both median values and a range indicating the 90% confidence interval. Monetized air quality impacts of naphthalene removal are similarly summarized in Table 3.

Table 2. Monetized climate benefits of naphthalene removal.

Impact Pathway	Impact (¢/gallon)
Black carbon radiative forcing (15% nvPM reduction)	0.09 (90% CI: 0.01 – 0.23)
Black carbon radiative forcing (40% nvPM reduction)	0.23 (90% CI: 0.04 – 0.61)
Contrail radiative forcing (15% nvPM reduction)	1.06 (90% CI: 0.30 – 2.59)
Contrail radiative forcing (40% nvPM reduction)	2.77 (90% CI: 0.77 – 6.89)
Hydrotreating CO_2 emissions	-1.82 (90% CI: -0.30 – -4.70)
Extractive distillation CO_2 emissions	-1.89 (90% CI: -0.31 – -5.01)
Sulfate aerosol (hydrotreating only)	-4.17 (90% CI: -0.61 – -11.23)

Table 3. Monetized air quality benefits of naphthalene removal.

Impact Pathway	Impact (¢/gallon)
nvPM emissions (15% nvPM reduction)	0.04 (90% CI: 0.02 – 0.06)
nvPM emissions (40% nvPM reduction)	0.11 (90% CI: 0.06 – 0.16)
Sulfur emissions (hydrotreating only)	1.92 (90% CI: 1.04 – 2.76)

Outreach Efforts
- ASCENT advisory board presentations (October 2018, October 2019)
- Presentation at the CAEP/12-WG3/2 meeting (October 2019) titled "Economic and Environmental Assessment of Jet Fuel Naphthalene Removal"

Student Involvement

This task was conducted primarily by Drew Weibel, working directly with Prof. Steven Barrett and Dr. Raymond Speth.

References
Brem, B.T., Durdina, L., Siegerist, F., Beyerle, P., Bruderer, K., Rindlisbacher, T., Rocci-Denis, S., Andac, M.G., Zelina, J., Penanhoat, O., & Wang, J. (2015). Effects of fuel aromatic content on nonvolatile particulate emissions of an in-production aircraft gas turbine. *Environmental Science & Technology,* 49, 13149–57.

Burkhardt, U., Bock, L., & Bier, A. (2018). Mitigating the contrail cirrus climate impact by reducing aircraft soot number emissions. *Climate and Atmospheric Science,* 1, 37.

Caiazzo, F., Agarwal, A., Speth, R.L., & Barrett, S.R.H. (2017). Impact of biofuels on contrail warming. *Environmental Research Letters,* 12, 114013.

Dedoussi, I.C. & Barrett, S.R.H. (2014). Air pollution and early deaths in the United States. Part II: Attribution of PM2.5 exposure to emissions species, time, location and sector. *Atmospheric Environment* 99, 610–7.

DeWitt, M.J., Corporan, E., Graham, J. & Minus, D. (2008). Effects of aromatic type and concentration in Fischer−Tropsch fuel on emissions production and material compatibility. *Energy & Fuels*, 22, 2411–8.

Mahashabde, A., Wolfe, P., Ashok, A., Dorbian, C., He, Q., Fan, A., Lukachko, S., Mozdzanowska, A., Wollersheim, C., Barrett, S.R.H., Locke, M., & Waitz, I.A. (2011). Assessing the environmental impacts of aircraft noise and emissions. *Progress in Aerospace Sciences*, 47, 15–52.

Punger, E.M. & West, J.J. (2013). The effect of grid resolution on estimates of the burden of ozone and fine particulate matter on premature mortality in the USA. Air Quality, *Atmosphere & Health*, 6 563–73.

Task 8 - Conduct Integrated Cost-Benefit Analysis of Impacts of Naphthalene Removal in the United States
Massachusetts Institute of Technology

Objective
The objective of this task is to produce an integrated cost-benefit analysis of naphthalene removal in the United States, accounting for the additional refining cost as well as the air quality and climate impacts.

Research Approach
The overall cost-benefit assessment of naphthalene removal includes fuel production costs, air quality benefits, and climate impacts from fuel production and fuel consumption. Fuel production costs were evaluated in tasks that were completed in previous project years. Air quality benefits and non-contrail climate impacts were calculated per unit reduction in nvPM mass and number emissions, based on the results of Grobler et al. (2019). These impacts are then scaled using the emissions reductions determined in the results of Task 1. Contrail impacts are estimated based on contrail modeling studies which investigated the effect of reductions in the soot number emissions index (Caiazzo et al., 2017; Bier & Burkhardt, 2019). Finally, all effects are placed on a common monetized basis to compare different naphthalene removal scenarios. We consider uncertainties in the assessment of each component and use these uncertainties to compute the likelihood of a net benefit for different scenarios.

Milestone
The work completed for this task was documented in Deliverable 2-5, provided to the FAA on July 31, 2018.

Major Accomplishments
The processing costs, air quality benefits, and climate impacts of naphthalene removal are converted to a common basis of cents per liter, as presented in Table 4. The benefits of widespread naphthalene removal are outweighed by the costs of processing the fuel and the CO_2 emissions associated with that processing.

Table 4. Costs (positive) and benefits (negative) of naphthalene removal.

	Component	Hydrotreatment (¢/liter)		Extractive Distillation (¢/liter)	
		Median	95% CI	Median	95% CI
Processing	Refinery	2.4	2.0 – 2.7	1.7	1.5 – 2.0
Air quality	nvPM	-0.004	0 – -0.01	-0.009	0 – -0.03

	Fuel sulfur	-0.51	-0.28 – -0.73	0	
Climate	nvPM	-0.02	0 – -0.04	-0.04	-0.01 – -0.09
	Fuel sulfur	1.06	0.15 – 2.85	0	
	Contrails	-0.16	-0.04 – -0.44	-0.38	-0.09 – -1.0
	Refinery CO_2	0.46	0.08 – 1.19	0.48	0.08 – 1.27
Total		**3.2**	**2.2 – 4.7**	**1.8**	**1.0 – 2.5**

For hydrotreatment, the climate impacts of the refinery CO_2 emissions exceed the expected air quality and climate benefits associated with the reduction in soot emissions. Furthermore, the net present value of the climate warming associated with sulfur removal is greater than the NPV of the reduced air-quality-related damages. For extractive distillation, the median air quality and climate benefits are approximately equal to the societal cost of the refinery CO_2 emissions. In addition to these environmental costs, the costs associated with processing jet fuel in the refinery must also be considered. These results suggest that, in the absence of a strong contrail effect, naphthalene removal on a nationwide basis is unlikely to be cost beneficial using either extractive distillation or hydrotreatment. However, it may be possible that naphthalene removal could be beneficial under certain circumstances, e.g., if applied to fuels used at individual airports with particular air quality concerns, or if used at times in locations where the formation of net warming contrails is most likely.

Outreach Efforts
- ASCENT advisory board presentations (April 2017, April 2018, October 2018, October 2019)
- Presentation at the CAEP/12-WG3/2 meeting (October 2019) titled "Economic and Environmental Assessment of Jet Fuel Naphthalene Removal"
- Presentation to the Aviation Emissions Characterization (AEC) Roadmap annual meeting (May 2020)

Student Involvement
This task was conducted primarily by Drew Weibel, working directly with Prof. Steven Barrett and Dr. Raymond Speth.

References
Bier, A., & Burkhardt, U. (2019). Variability in Contrail Ice Nucleation and Its Dependence on Soot Number Emissions. *Journal of Geophysical Research: Atmospheres*, *124*(6), 3384–3400. https://doi.org/10.1029/2018JD029155

Caiazzo, F., Agarwal, A., Speth, R. L., & Barrett, S. R. H. (2017). Impact of biofuels on contrail warming. *Environmental Research Letters*, *12*(11), 114013. https://doi.org/10.1088/1748-9326/aa893b

Grobler, C., Wolfe, P. J., Dasadhikari, K., Dedoussi, I. C., Allroggen, F., Speth, R. L., Eastham, S. D., Agarwal, A., Staples, M. D., Sabnis, J., & Barrett, S. R. H. (2019). Marginal climate and air quality costs of aviation emissions. *Environmental Research Letters*, *14*(11), 114031. https://doi.org/10.1088/1748-9326/ab4942